universität wien

# MASTERARBEIT | MASTER'S THESIS

Titel | Title

Enzyme Mechanisms Beyond Oxygen Rebound: Synthesis of Isotopically Labelled DfmD, FfnD and TmpA Substrates and Biochemical Study.

verfasst von | submitted by

Sebastian-Felix Fritz BSc

angestrebter akademischer Grad | in partial fulfilment of the requirements for the degree of

Master of Science (MSc)

Wien | Vienna, 2024

| | |
|---|---|
| Studienkennzahl lt. Studienblatt \| Degree programme code as it appears on the student record sheet: | UA 066 862 |
| Studienrichtung lt. Studienblatt \| Degree programme as it appears on the student record sheet: | Masterstudium Chemie |
| Betreut von \| Supervisor: | Dr. Katharina Pallitsch Privatdoz. Bakk. MSc |

# Acknowledgements

Am Ende meines Studiums könnte ich einen ganzen Hörsaal mit den Leuten füllen, denen ich nicht genug danken kann.

An erster Stelle möchte ich hierbei meiner Betreuerin, Chefin, Kollegin und manchmal auch Leidensgenossin Katharina Pallitsch danken die mich aufgenommen hat und es irgendwie geschafft hat einen waschechten Phosphor-Synthesechemiker aus mir zu machen. Auch wenn es hin und wieder stressig war und die Chemie nicht wollte, hast du mich immer unterstützt und mich immer motiviert meiner Intuition zu folgen, sodass wir zum Schluss doch noch jedes Ziel zumindest im Blick hatten! Vielen Dank Kathi!

Auch wenn wir nur kurz das Labor und das Büro teilen durften so bin ich außerdem überaus dankbar für die Zusammenarbeit mit Tamara Dinhof ohne die ich mich wahrscheinlich bis heute nicht im Labor (und in meinem Laborjournal) zurechtfinden würde. Ohne deinen Input wäre Vieles schwieriger gewesen und vor allem auch wahrscheinlich ein bisschen weniger lustig! Danke Tami, dass du mich in eurem Labor so willkommen geheißen hast! Danke auch an Niko und Kristof, die nicht nur ein Quell an Fachliteratur und Reaktionen sind, sondern auch jeden noch so stinkigen, trüben, verregneten, heißen, … Labortag zu einem lustigen Arbeitstag gemacht haben!

Ein besonderer Dank gilt auch den Studierenden, die ich im Labor betreuen durfte, allen voran Naomi! Ohne deine motivierte und kreative Mitarbeit wäre vieles von dem, was ich in meiner Zeit hier erarbeiten durfte, nicht möglich gewesen. Die Zusammenarbeit mit dir war unglaublich motivierend und ich bin stolz dein Co-Betreuer gewesen zu sein. Jede Arbeitsgruppe die dich als Mitarbeiterin hat, darf sich glücklich schätzen! Zudem möchte ich meinem Ersti und Ersthelfer Flo danken; auch wenn Glasgeräte mal auf unübliche Art und Weise in Aktion waren so konnte ich mich auf deine Hilfe verlassen! Danke!

Abseits des Labors gibt es aber natürlich noch eine ganze Reihe an Personen ohne die die letzten Jahre wohl ganz anders ausgeschaut hätten. Danke meinen Studienkollegen

Amanda, Magnus, den Philipps und Max. Ohne euch wären die letzten Jahre wohl weniger erfolgreich gewesen! Danke Magnus, ohne deine Hilfe hätte diese Arbeit ein kleines bisschen anders ausgeschaut! Danke dass ihr da seid und da wart!

An dieser Stelle möchte ich auch der Arbeitsgruppe von J. Martin Bollinger Jr. und Carsten Krebs danken die mich bei sich aufgenommen haben und mich in die Welt der Enzymkinetik eintauchen haben lassen. Hierbei möchte ich besonders Brandt Graham danken mit dessen Unterstützung diese Arbeit zu einer interdisziplinären Arbeit werden konnte!

Last but not least möchte ich auch Simon und meiner Familie danken. Ohne eure Unterstützung in den vergangenen Jahren hätte ich dieses Studium wohl nie zu Ende bringen können. Danke Mama und Papa, dass ihr mich in meinen Entscheidungen immer unterstützt! Danke auch dir Theresa, ohne dich als Vorbild hätte ich wahrscheinlich nie ein Studium begonnen! Danke Stefanie für die vielen großartigen Ablenkungen, die mich jedes Mal erwarten, wenn ich heim in die Steiermark fahre! Und ohne dich Simon wäre weder diese Arbeit jetzt fertig, noch hätte ich die Motivation gehabt so lange mit dem Deuterium zu kämpfen!

**Vielen Dank!**

# Content

## List of Abbreviations

***(***

(*S*)-MTPACl ..... *(S)-(+)-Methoxy-trifluomethylphenylacetyl-chlorid; Mosher's acid chloride*

***2***

2-AEP .....*2-aminoethylphosphonic acid*

2OG ..... *2-oxoglutaric acid*

***A***

Ar .....*Argon*

ATD ..... *asymmetric transfer deuteration*

ATP .....*adenosine-5'-triphosphate*

***C***

CSAs..... chiral solvating agents

***D***

DCM .....*dichloromethane*

DIP.....*dissolved inorganic phosphorus*

DOP .....*dissolved organic phosphorus*

***E***

$E_a$ .....*activation energy*

***H***

HAEP.....*(R)-2-amino-1-hydroxy-ethylphosphonate*

HPLC ..... *high-performance liquid chromatography*

***K***

KIE ..... *kinetic isotope effect*

***L***

LAD.....lithium aluminium deuteride

***M***

MPLC .....*medium pressure liquid chromatography*

MRM ..... *multiple reaction monitoring*

***N***

NMR.....*nuclear magnetic resonance*

***P***

PepM.....*phosphoenolpyruvate mutase*

***R***

RNA ..... *ribonucleic acid*

***S***

SIM ..... *single ion monitoring*

***T***

TADDOLs.....(4R,5R)-2,2-Dimethyl-α,α,α',α'-tetraphenyl-dioxolan-4,5-dimethanol

TDP .....total dissolved phosphorus

THF ..... *tetrahydrofuran*

# 1. Introduction

## 1.1. Phosphorus in Nature

Phosphorus is an essential element for all living organisms; still, the global phosphorus biogeochemical cycle has only received little attention in recent decades. While more than 32,000 papers on all aspects of the global carbon cycle, and more than 12,000 papers on all aspects of the global nitrogen cycle can be found between 2000 and 2024, less than 2,500 papers covering phosphorus cycling were published in the same period.[1]

Typical forms of inorganic phosphorus in nature are phosphates, *e.g.,* $PO_4^{3-}$, $HPO_4^{2-}$, $H_2PO_4^{-}$, or phosphoric acid ($H_3PO_4$). In contrast to other essential elements, gaseous forms of phosphorus, *e.g.,* phosphine ($PH_3$), are rare.[2]

The phosphorus cycle is the slowest terrestrial biogeochemical cycle, characterised by a time-limiting step, the tectonic movement of phosphorus-containing rock to the surface, that spans approximately 500 million years. Unlike the global nitrogen and carbon cycle, it does not involve the atmosphere. Instead, phosphorus primarily circulates through the lithosphere, hydrosphere, and biosphere. The main source of phosphorus is the weathering of phosphate-containing rocks. This term describes the entity of all chemical and physical processes acting on phosphorus-containing minerals *e.g.* apatite which lead to a release of phosphate into the environment. The released phosphorus is then adsorbed to positively charged sites of sediment particles as phosphate ions. Additionally, the transportation by surface- and ground-freshwater bodies into the oceans is a form of phosphorus release into these ecosystems. Plants and algae can take up phosphate from water and soil to form organic and inorganic phosphorus-containing compounds which are the main source of phosphorus for *animalia*. *Via* mineralisation, decomposition and excretion, animals release phosphorus again to the soil. However, the major part of the particulate forms of phosphorus never enters the biosphere, instead, it forms sediments in the ocean before being lifted to the surface again by geological forces.[2]

The phosphorus cycle has been highly influenced by mankind since the industrial revolution. Agriculture, mining, fertilisation and soil erosion increased the movement of phosphorus around the planet. The overuse of phosphorus-containing fertilizers in agriculture might lead to phosphorus scarcity in the near future. With population growth, the demand for phosphorus-based fertilizers steadily increases. In 2009, estimations suggested that the peak of phosphorus production would be reached around 2030. However, with new apatite reserves found in Morocco, the Western Sahara territory, and Algeria, an estimation of the globally available phosphorus is hardly possible.[2,3] Still, phosphorus scarcity is likely to impact global food production in the near future.

This excessive use of phosphorus-based fertilisers in agriculture also has significant environmental consequences, particularly for the hydrosphere. Over-enrichment of aquatic ecosystems with phosphorus leads to eutrophication in lakes, rivers, and estuaries, which promotes the proliferation of algae and cyanobacterial blooms. Phosphorus tends to be retained efficiently in these aquatic systems, resulting in elevated primary production, particularly during summer and autumn. Increased primary production subsequently leads to high rates of organic matter decomposition, causing significant depletion of dissolved oxygen in bottom and surface waters alike, especially during calm nighttime conditions. These eutrophic conditions can trigger fish kills and drive substantial shifts in species composition across all trophic levels. This ultimately leads to reduced biodiversity and altered ecosystem stability as proven by researchers at the Experimental Lakes research area in northwestern Ontario.[4]

## 1.2. Inorganic Phosphorus in higher biological Systems

Phosphorus plays varied roles in all species. In higher biological systems, phosphodiester bonds between mononucleotide units enables the formation of long DNA and RNA chains, facilitating the replication and transmission of genetic information. Additionally, phosphorus is an integral component of cellular energy transfer by the conversion of adenosine-5’-triphosphate (ATP) to adenosine-5’-diphosphate (ADP), which releases energy, essential for many metabolic processes. Although the total phosphorus content in

living systems is relatively small compared to nitrogen and carbon, its plays a crucial role in the metabolism of all known life forms.[2,3,5] Phosphorus primarily exists as inorganic phosphate in the lithosphere and hydrosphere. Consequently, higher organisms, such as vertebrates and molluscs, can utilise phosphorus exclusively in the form of phosphate. The majority of inorganic phosphate in the human body (estimated 85 % of the total inorganic phosphate) occurs as insoluble hydroxyapatite [$Ca_5(PO_4)_3(OH)$] or as its dimer **1** [$Ca_{10}(PO_4)_6(OH)_2$], primarily found in bone and teeth.[6] (Figure 1)

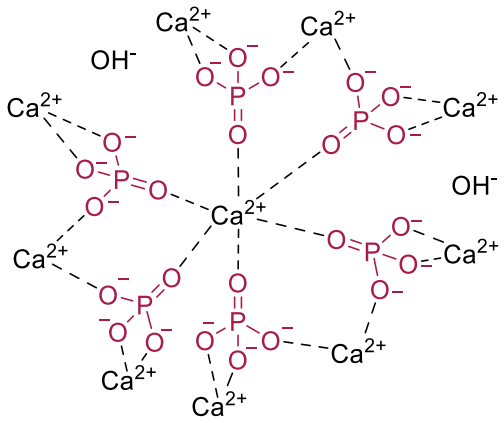


**1**

Figure 1 Hydroxyapatite in its dimeric form.

Phosphoric acid is the primary source of all inorganic phosphate salts in biological systems. With a pKa of 2.16, phosphoric acid has a higher acidity than other biologically relevant acids, such as citric acid (pKa 3.13) and acetic acid (pKa 4.76). Consequently, all phosphate-containing molecules (inorganic and organic) are negatively charged at physiological pH.[6]

## 1.3. Organophosphorus Compounds

While not being a suitable phosphorus source for higher organisms, various organophosphorus compounds still play important roles within the biosphere. Among these, organic phosphate esters, phosphinates and phosphonates stand out significantly

and play crucial roles in biological systems. Trialkyl phosphines, trialkyl phosphites and phosphine oxides of minor biological relevance will not be addressed in this chapter.[2,6,7]

### 1.3.1. Phosphoric Acid Derivatives $PO_4^{3-}$

Phosphoric acid derivatives, including phosphate esters, anhydrides, and pyrophosphoric acid esters, are the prevalent organophosphorus compounds in most biological systems. Phosphate-based molecules, such as ATP (**2**), phosphoenolpyruvate (**4**), and creatine phosphate (**5**), serve as primary chemical energy sources within these systems. (Figure 2) Furthermore, DNA and RNA molecules (exemplified **3**), contain a phosphoric acid diester backbone. These phosphoric acid diesters serve as the target sites for nucleotidyl transferases, such as DNA and RNA polymerases. Consequently, they play a crucial role in the chain elongation processes of DNA and RNA synthesis and repair.[6,7]

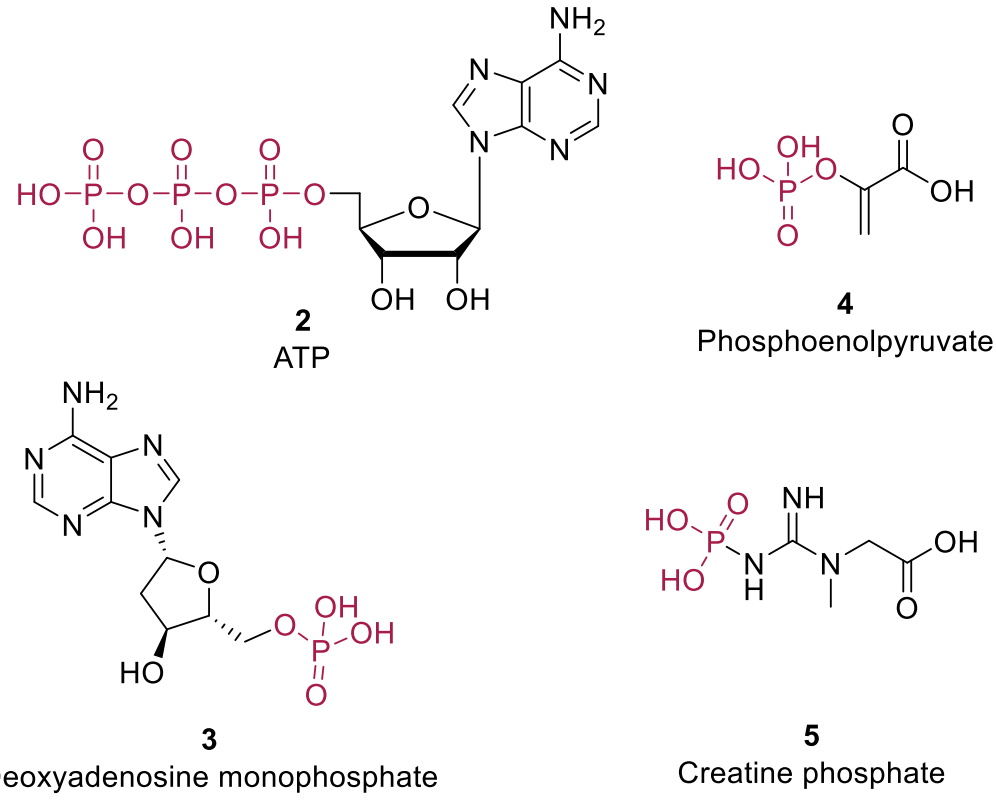


Figure 2 Structures of ATP, creatine phosphate, phosphoenolpyruvate and deoxyadenosine monophosphate (as example for DNA and RNA substructures).[6]

Apart from the mentioned small molecules, phosphoric acid derivatives also play a crucial role as cell structural components in the form of phospholipids, phosphoglycanes and in phosphosphingomyelines. These compounds all contain a glycerol backbone connected to a fatty acid, which is coupled to a hydrophilic head group *via* a phosphodiester moiety.[8,9] (Figure 3)

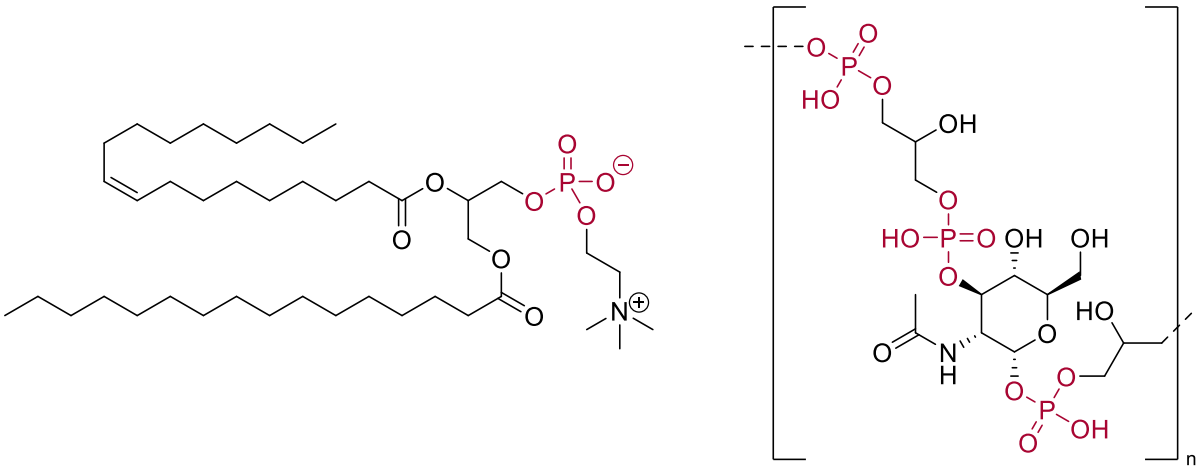

**6**
1-oleoyl-2-palmitoyl-phosphatidylcholine

**7**
Teichoic acid repeat unit

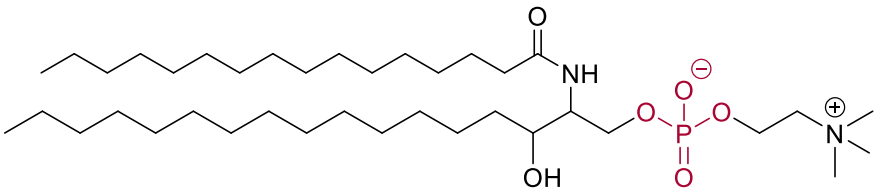

**8**
Sphingomyelin

Figure 3 Structures of 1-oleoyl-2-palmitoyl-phosphatidylcholin (**6**) (as an example for phospholipids), Teichoic acid (**7** as example for a phosphonoglycan) and Sphingomyelin (**8** as an example for a phosphosphingomyelin).

### 1.3.2. Phosphinates $R_2PO_2^-$

Phosphinates are structurally similar to phosphate esters, but two P–O bonds are replaced by direct C-P bonds, making these molecules more stable against harsh chemical conditions (*e.g.*, acids and bases, thermal or enzymatic degradation). The most prominent phosphinates are probably the naturally occurring phosphinothricin antibiotics bialaphos **9** (a tripeptide consisting of 2 alanine molecules and the non-proteinogenic amino acid phosphinothricin) or trialaphos (the corresponding tetrapeptide with 3 alanines and phosphinothricin). These naturally occurring antibiotics can be found in different organisms such as *Streptomyces hygroscopicus* or *Streptomyces viridochromogenes*. (Figure 4). The phosphinothricin moiety works as a structural analogue of glutamate and works as an inhibitor of glutamine synthetase in bacteria. While phosphinothricin on its own is believed to be poorly taken up by bacterial cells, connecting it to small amino acid sequences leads to better antibiotic results. Due to their structural similarity to phosphate esters, phosphinates can mimic the biological functions of these esters while offering greater resilience to chemical degradation. This also makes synthetic phosphinates significant for the development of new antibiotics, providing a promising pathway for creating new robust therapeutic agents.[10]

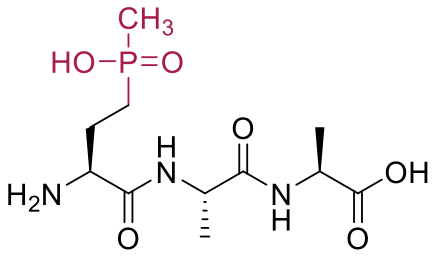


**9**
Bialaphos

Figure 4 Bialaphos (**9**) as an example of naturally occurring phosphinates

### 1.3.3. Phosphonates $RP(O)(OR)_2$ and Phosphonic Acids $RP(O)(OH)_2$

Phosphonates (the salts and esters of phosphonic acids) are a group of natural products that contain one direct P-C bond which makes them chemically, thermally and

enzymatically more stable than phosphate esters while being almost isosteric to the latter. The intrinsic P-C bond makes these molecules stable against hydrolysis and resistant to the enzymatic action of *e.g.* phosphatases.[6] Their biological relevance will be discussed in the following chapter.

## 1.4. Relevance of Phosphonic Acids in Nature

2-Aminoethyl-phosphonate (**10**, 2-AEP) was the first phosphonate to be found in nature and was discovered in sheep rumen ciliate protozoa in 1959. These protozoa enrich their membranes with 2-AEP as polar head group to withstand the harsh conditions of the sheep rumen. Today we know that phosphonic acids and the corresponding organophosphonates are produced by a variety of bacteria and archaea.[6,11]

The use of organophosphonates as polar head groups in cell membrane components is believed to protect marine microorganismal cell walls against hydrolysis. While many phosphonates play crucial roles as macromolecular conjugates in biological systems, some microbial species also produce low molecular organophosphonates that display very interesting drug-like properties. Some of these acts as antibiotics or have herbicidal properties. Today we know approximately 40 low molecular microbial metabolites that contain a C-P bond. A comparably high share of which exhibit the previously discussed (Chapter 1.3) properties. [6,11]

Apart from their interesting bioactivity spectrum, phosphonates are of special scientific interest due to their role in the global phosphorus cycle. While higher organisms solely rely on phosphates and phosphate esters as P-source, the microbial world is not only able to produce phosphonates as structural components, but also to use them as alternative phosphorus source. The ability to use phosphonates might present an evolutionary advantage in phosphate-depleted environments. This is especially relevant in aquatic ecosystems regarding the low solubility of phosphates at ambient pressure, temperature and pH. Therefore, the availability of phosphorus is typically described in terms of total dissolved phosphorus (TDP), which is the combined amount of all dissolved organic and inorganic phosphorus species (DOP, up to 80 % of TDP in the surface layer of oligotrophic gyres) and (DIP). It is estimated that approximately 25% of the dissolved organic phosphorus in the hydrosphere consists of organophosphonates, with 2-aminoethyl-phosphonate (2-AEP) and methylphosphonate being the most prevalent compounds. This highlights the importance of understanding the enzymatic processes involved in the

formation and degradation of phosphonates. Such knowledge is essential for gaining a better understanding of the global phosphorus cycle.[2,3,11–13]

## 1.5. Overview of the Phosphonate biosynthetic Pathways

The biosynthesis of nearly all known naturally occurring phosphonates starts with the rearrangement of phosphoenolpyruvate (**4**) into phosphonopyruvate (**11**), forming the carbon-phosphorus (C-P) bond. This reaction is catalysed by the enzyme phosphoenolpyruvate mutase (PepM). The equilibrium of this initial step heavily favours the substrate (phosphoenolpyruvate) over the product (phosphonopyruvate) by approximately 500-fold. To drive the equilibrium towards product formation, a subsequent irreversible reaction is employed, effectively trapping phosphonopyruvate and facilitating the biosynthesis of varied phosphonates.[14,15]

Currently, four known subsequent enzymatic reactions are known to divert phosphonopyruvate to different metabolic routes (Scheme 1): (1) decarboxylation by phosphonopyruvate decarboxylase (Ppd) yielding phosphonoacetaldehyde (**12**); (2) transamination by a pyridoxal 5'-phophate-dependent aminotransferase (*e.g.* PalB) yielding phosphonoalanine (**13**); (3) reduction by an NAD(P)H-dependent dehydrogenase yielding phosphonolactate (**14**); and (4) an aldol-like condensation with acetyl-CoA catalysed by phosphonomethylmalate synthase (PMSy) yielding phosphonomethylmalate (**15**). Due to the inherently reversible nature of transaminations, phosphonoalanine (**13**) must be sequestered, for instance by attachment to a lipid or glycan, to drive the biosynthetic pathway forward.

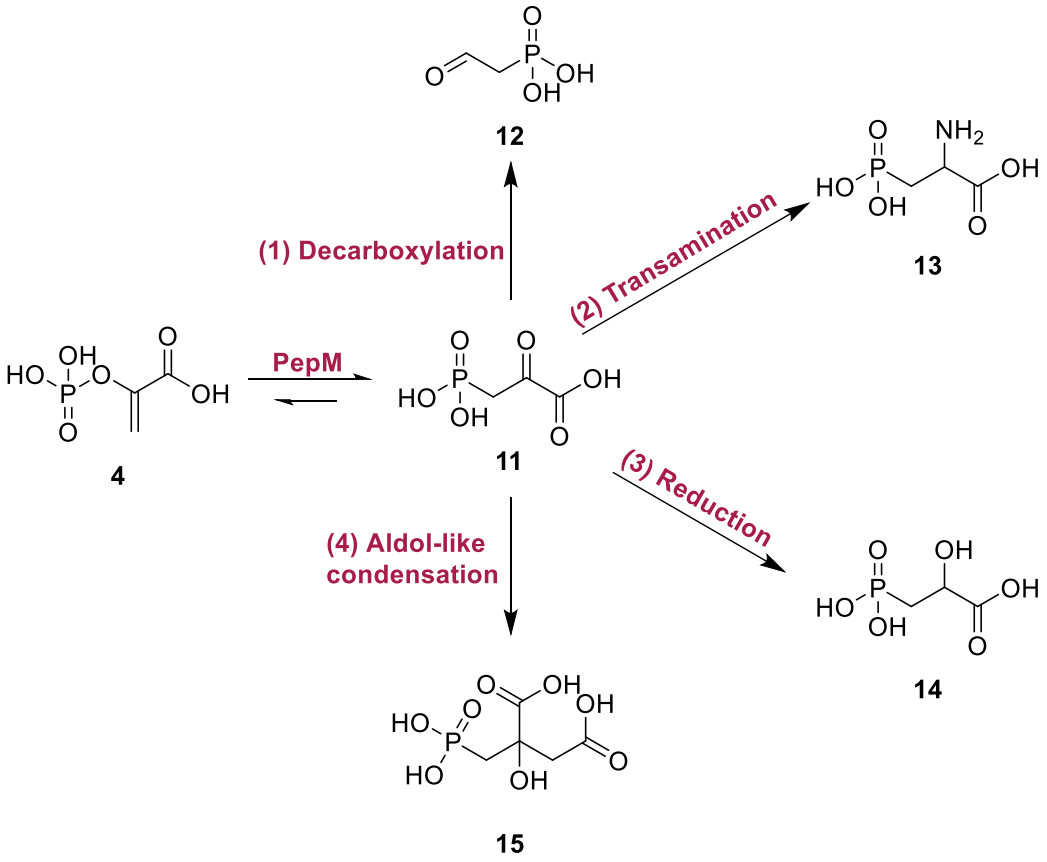


Scheme 1 Overview of the common first step of the biosynthesis of phosphonate synthesis and the subsequent reactions.

Phosphonoacetaldehyde (**12**) is recognized as an important intermediate and branching point in the biosynthesis of several notable compounds, including phosphinothricin, fosfonochlorin, fosfomycin, and dehydrophos. Many of the subsequent unique transformations during the biosynthesis of these compounds are catalysed by highly specialized, oxidative enzymes. Among these, non-heme iron(II) and 2-oxoglutarate-dependent oxygenases (Fe(II)/2-OG oxygenases) play an outstanding role. [15]

## 1.6. Non-heme Iron(II) and 2-oxoglutarate-dependent Oxygenases in the Biosynthesis of Phosphonates

Non-heme iron (II) and 2-oxoglutarate-dependent oxygenases are highly versatile and catalyse a broad spectrum of biochemical transformations. They are known for their exceptional chemo- and stereoselectivity. These enzymes employ 2-oxoglutarate as a co-substrate in conjunction with molecular oxygen. Within the active site, the Fe(II) ion is typically converted into a highly reactive ferryl species (Fe(IV)=O), which facilitates the abstraction of an α-hydrogen from the substrate, generating a substrate radical and ferric hydroxide. In most cases, the substrate radical then reacts with oxygen, resulting in the hydroxylation of the substrate through a mechanism known as "oxygen rebound". The first enzyme of this superfamily identified in connection with phosphonate metabolism was PhnY*. PhnY* specifically catalyses the hydroxylation of 2-aminoethylphosphonate (**10**, 2-AEP) to produce (*R*)-2-amino-1-hydroxy-ethylphosphonate (**16**, HAEP).

However, other enzymes of this types, divert the intermittently formed substrate radical to other chemistry. FfnD for example catalyses an epoxide formation with a preinstalled substrate hydroxyl group during the biosynthesis of fosfonochlorin; DhpJ catalyses the desaturation during the biosynthesis of dehydrophos, and DfmD catalyses the desaturation and the chain elongation *via* demethylation during the biosynthesis of FR-32863. (Scheme 2)[15] For this work, the mechanisms of FfnD and DfmD are particularly interesting.

1) PhnY*/TmpA catalysed hydroxylation

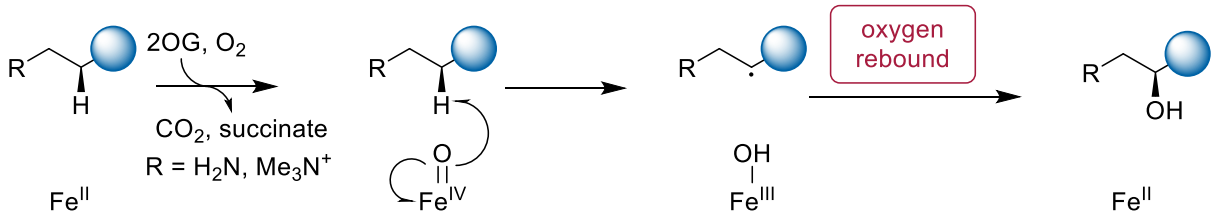


2) FfnD catalysed oxacyclisation of 2-hydroxyethylphosphonic acid

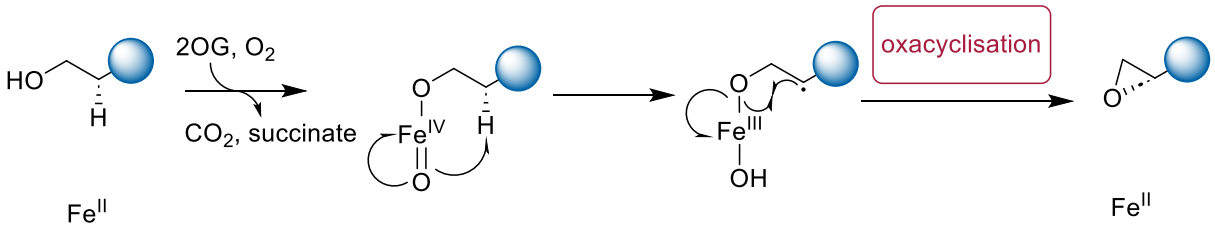


3) DhpJ catalysed desaturation

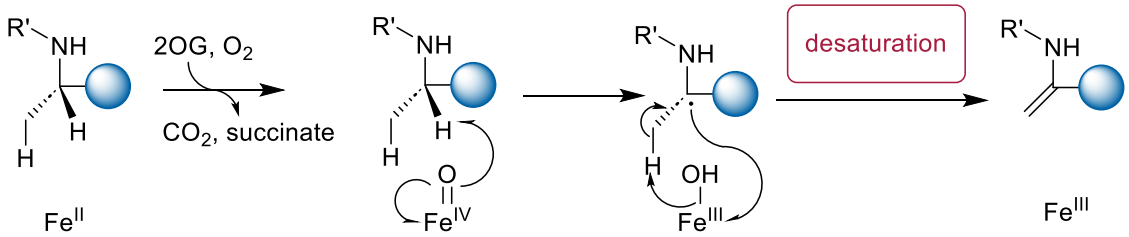


4) DfmD catalysed desaturation and chain elonfation/demethylation of *N,N,N*-trimethylphosphonic acid

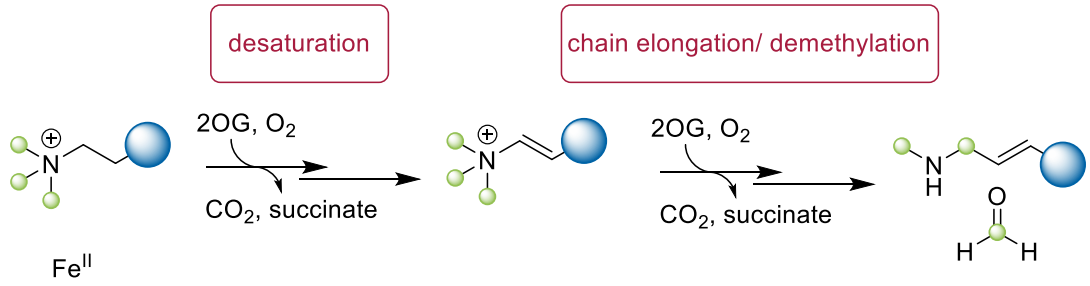


Scheme 2 Overview of different transformations catalysed by non-heme iron(II) and 2-oxoglutarate-dependent oxygenases. $P(O)(OH)_2$ groups are depicted as blue spheres and *N*-methyl and methylene groups are depicted with green spheres.[15]

# 2. Aims of the Thesis

This interdisciplinary master's thesis in the field of bioorganic chemistry focuses on the synthesis of deuterated substrate-analogues for the non-heme iron(II) and 2-oxoglutarate-dependent oxygenase DfmD, FfnD and TmpA. These will be used in enzyme assays to study the mechanistic details of the catalysed reactions with a special focus on the underlying principles that allow DfmD and FfnD to omit oxygen rebound in favour of other reactions. (Figure 5)

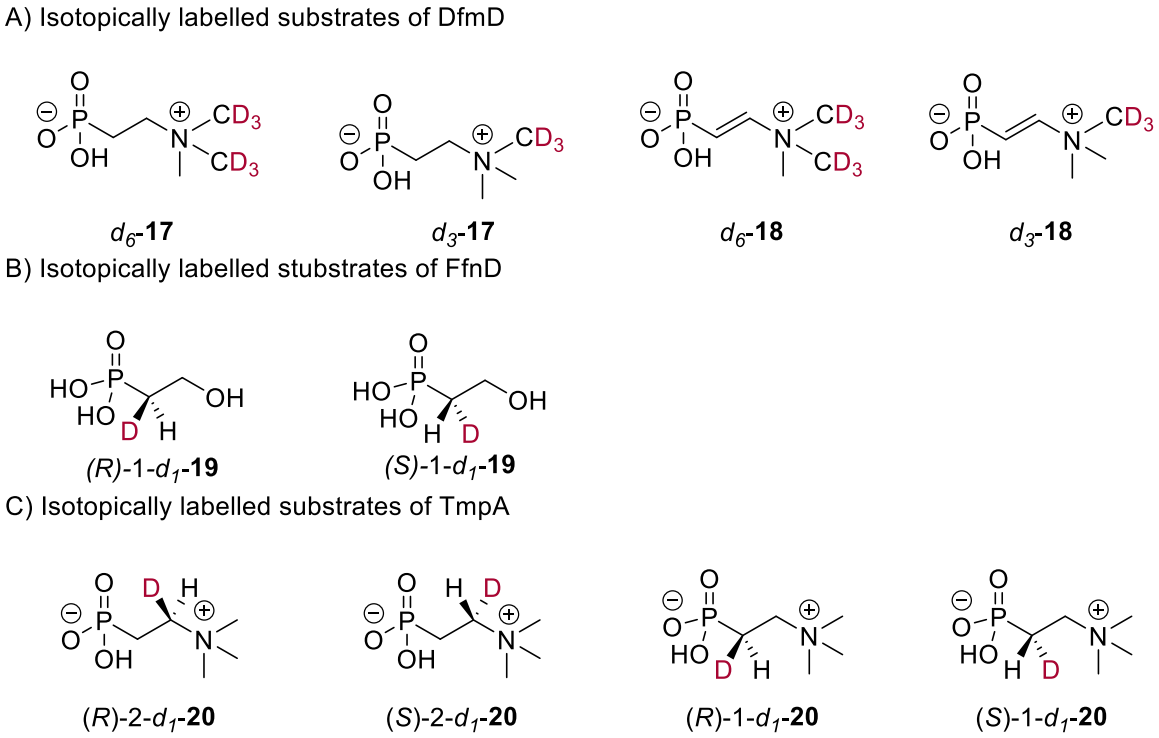


Figure 5 Overview of the chemical structures of the target molecules.

This study aims to develop reproducible and purely chemical synthetic sequences for the production of the target compounds, with a focus on achieving consistently high enantioisotopic purities, while using cheap deuterium sources and atom economic methods. Although two of these molecules ( (*R*)-2-$d_1$-**19** and (*S*)-2-$d_1$-**19**) were previously synthesized through a chemoenzymatic approach by Hammerschmidt *et al.* (1991, 11

steps using NAD(D)$^+$ as a deuterium donor) a more atom economic synthesis is needed.[16,17] Two different approaches are going to be tested to incorporate deuterium into the substrates of FfnD (compounds (*R*)-1-$d_1$-**19** and (*S*)-1-$d_1$-**19**) and TmpA (compounds (*R*)-1-$d_1$-**20,** (*S*)-1-$d_1$-**20,** (*R*)-2-$d_1$-**20** and (*S*)-2-$d_1$-**20**). The preferential method will be an asymmetric transfer deuteration for the reduction of aldehydes *via* a Noyori-type catalyst with DCOOH as stoichiometric deuterium source. If the first approach fails to give the desired products in satisfying yields and enantiomeric purities, secondly, the reduction of deuterated aldehydes with different commercially available borane reagents (in combination with CBS catalysts) or Alpine borane® will be tested. The DfmD substrate analogues (compounds $d_6$-**17**, $d_3$-**17,** $d_6$-**18** and $d_3$-**18**) will be synthesised according to procedures known for the synthesis of the unlabelled compounds .[18]

The second part of the thesis will focus on enzymatic studies on the mode of action of FfnD, TmpA and DfmD using the generated substrates via stopped-flow methods, ESI-MS enzymatic assays and NMR enzymatic assays to gain a better understanding of the mechanistic principles that the target enzymes apply.

# 3. Methods

## 3.1. Proposed Synthesis

The following subchapter describes the proposed synthetic strategies to produce the desired compounds.

### 3.1.1. Proposed synthetic Strategy to access DfmD Substrates

The proposed synthesis of the saturated DfmD substrates $d_6$-**17** and $d_3$-**17** starts with an Arbuzov reaction of 1,2-dibromoethane (**21**) and triethyl phosphite (**22**). (Scheme 3) *N*-monomethylated phosphonate **24** can be synthesised by the addition of methylamine to **23**. The corresponding *N,N*-dimethylated compound **26** can be synthesised likewise by the addition of dimethylamine to **23**. $d_3$-Methyl iodine can then be used as a deuterium source to give the desired compounds $d_6$-**17** and $d_3$-**17** by methylation of **24** and **25** respectively, followed by deprotection and purification by ion exchange chromatography (IEC).

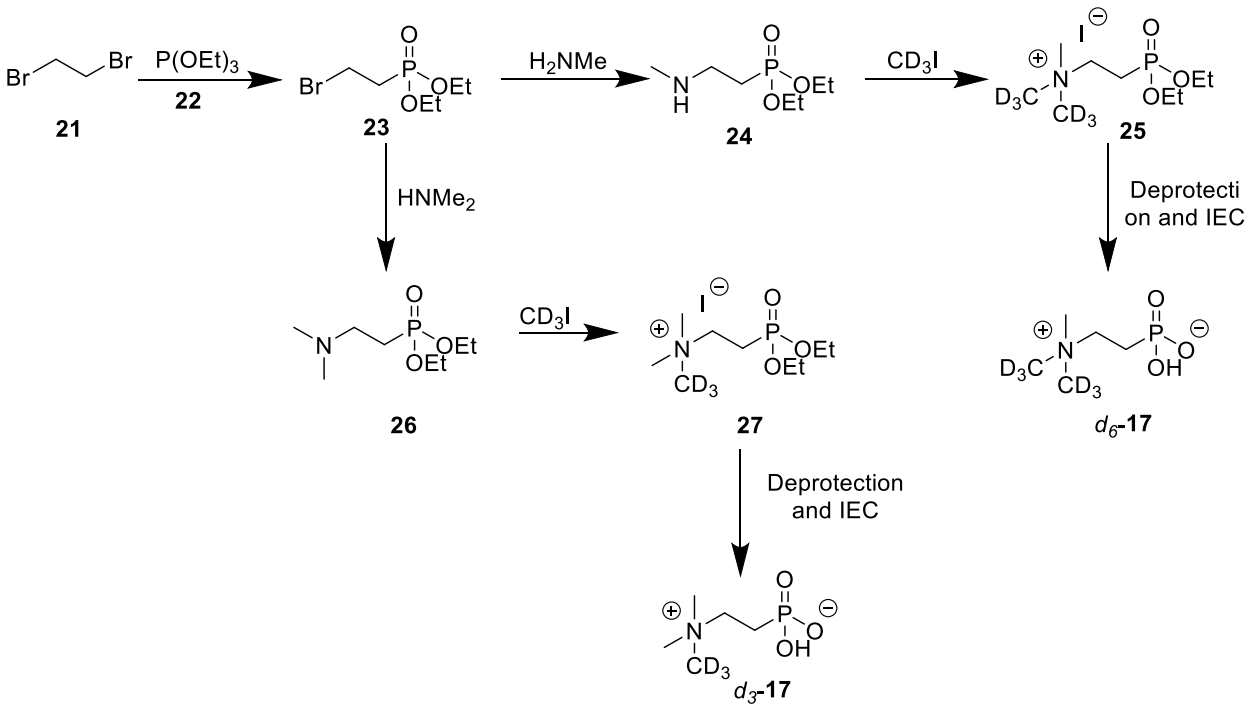


Scheme 3 Proposed strategy for the synthesis of the saturated DfmD substrates *d*$_3$-**17** and *d*$_6$-**17**.

The proposed synthesis of the unsaturated DfmD substrates *d*$_6$-**18** and d$_3$-**18** is planned analogously to the synthesis of the saturated DfmD substates *d*$_6$-**17** and *d*$_3$-**17**. However, instead of using 1,2-dibromoethane (**21**) as a starting material, 1,2-dibromoethylene (**28**) is going to be used. However, great care must be taken during the handling of intermediates **30** and **32**, as they are enaminophosphonates, which are typically very unstable (Scheme 4)

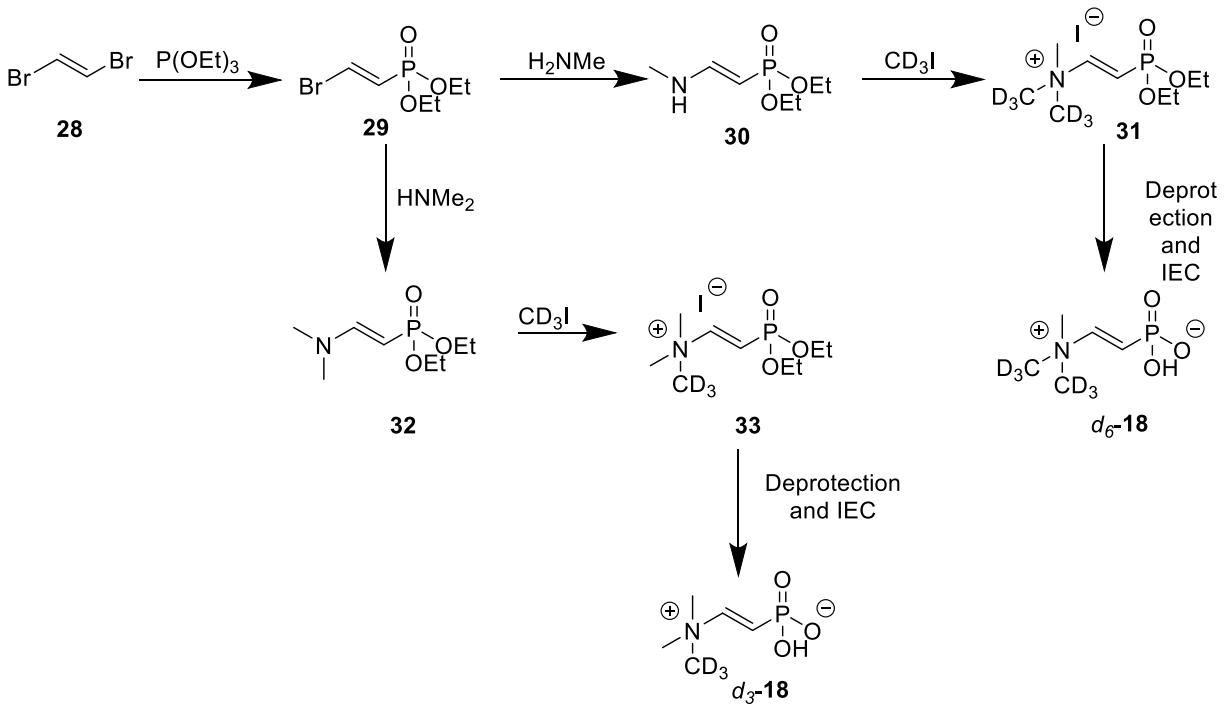


Scheme 4 Proposed synthetic strategy for the unsaturated DfmD substrates *d*$_3$-**18** and *d*$_6$-**18**.

### 3.1.2. Proposed synthetic Strategy to access FfnD and TmpA Substrates

The proposed synthesis of all four enantioisotopomers of compounds (*R*)-1-*d*$_1$-**19,** (*S*)-1-*d*$_1$-**19,** (*R*)-1-*d*$_1$-**20,** (*S*)-1-*d*$_1$-**20,** (*R*)-2-*d*$_1$-**20,** and (*S*)-2-*d*$_1$-**20** relies on the asymmetric reduction of suitable aldehydes as key step. Depending on the desired position of deuterium (at C-1 or C-2) in the final molecule, three different aldehydes can be envisaged as intermediates (**37**, **38**, **39**). The synthesis of **37** and **38** begins with 1-naphthyl methanol or phthalimide as starting material, respectively. Initially, phthalimide or 1-naphthyl methanol will be deprotonated with sodium hydride, followed by coupling with bromoacetaldehyde diethyl acetal. The subsequent deprotection of the diethyl acetals (**34** and **35**) is expected to yield the corresponding aldehydes **37** and **38**. For the synthesis of diethyl 2-oxoethylphosphonate (**39**), an Arbuzov reaction between triethyl phosphite and bromoacetaldehyde diethyl acetal at 180°C is proposed (see Scheme 5).

First attempts to introduce chirality will employ a Noyori-type catalyst, either (*R,R*)-**49** or (*S,S*)-**49**, in combination with DCOOH (*d*$_1$-**50**) and triethylamine as the deuterium source. This step is expected to directly yield the (*R*)- or (*S*)- mono-deuterated primary alcohols [(*R*)- or (*S*)-*d*$_1$-**40**, (*R*)- or (*S*)-**41,** (*R*)- or (*S*)-**42**] from the three key aldehydes.

An Appel-type reaction, involving carbon tetrabromide and triphenylphosphine ($PPh_3$) will be used to generate alkyl halides [(*R*)- or (*S*)-*d*$_1$-**43**, (*R*)- or (*S*)-**44,** (*R*)- or (*S*)-**45**] that can undergo Arbuzov-type reactions to ultimately obtain (*R*)- and (*S*)-*d*$_1$-**46** (from (*R*)- or (*S*)-*d*$_1$-**43**) and (*R*)- and (*S*)-*d*$_1$-**47** [from (*R*)- or (*S*)-*d*$_1$-**44**]. Like this, all possible enantioisotopomers (mono-deuterated at C-1) will become accessible after deprotection and methylation of the amino-group [the latter only for the synthesis of (*R*)- and (*S*)-*d*$_1$-**20**]. As both the Appel- and the Arbuzov reaction proceed under inversion of configuration, the deuterated alcohols [(*R*)- or (*S*)-1-*d*$_1$-**40**, (*R*)- or (*S*)-1-*d*$_1$-**41**]will ultimately give phosphonates of the same absolute configuration.

The synthesis of enantioisotopomers of **19** or **20**bearing a deuterium atom at C-2 will be attempted by asymmetric transfer deuteration of **39**. The resulting alcohols (*R*)- and (*S*)-*d*$_1$-**42** can again be converted to bromides and substitution of the latter will then again occur *via* an $S_N2$ reaction using either 1-naphthylmethanol or phthalimide to isolate the corresponding protected compounds (*R*)-2-*d*$_1$-**47**, (*S*)-2-*d*$_1$-**47**, (*R*)-2-*d*$_1$-**48**, (*S*)-2-*d*$_1$-**48**.

The final steps  for all compounds will be global deprotection, followed by purification of the free phosphonic acids using ion exchange chromatography, to afford the target compounds. (Scheme 5)

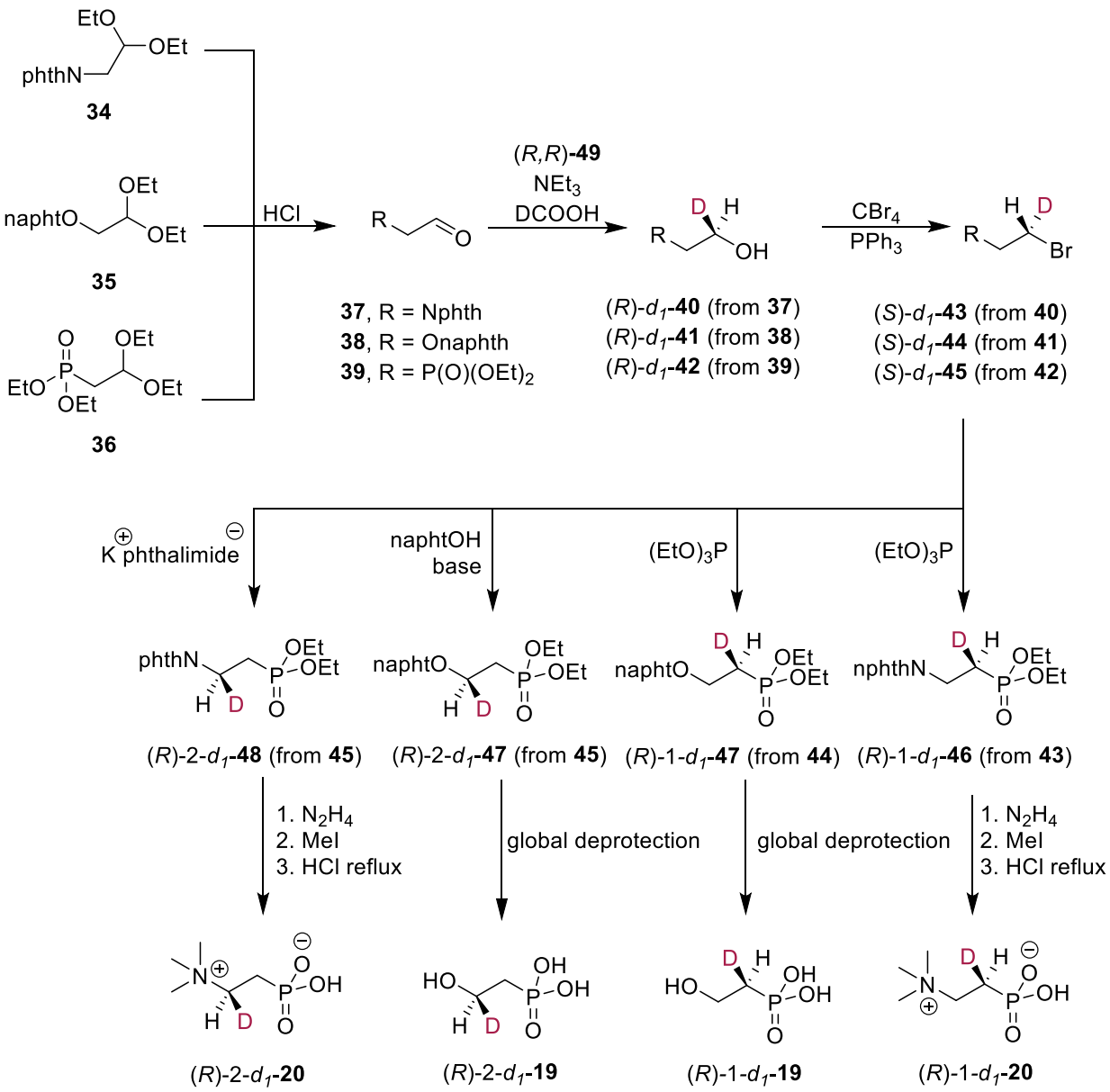


Scheme 5 Proposed synthesis route to yield the desired mono-deuterated substrates of FfnD and TmpA, exemplified for the respective (*R*)-enantiomers, obtained by using (*R,R*)-**49**. In order to synthesise the (*S*)-enantiomers, (*S,S*)-**49** will be used.

## 3.2. Known Methods for stereoselective Deuterations

### 3.2.1. Enzymatic Methods

The formation of chiral centres in natural products is highly optimized by enzymes. Thus, the use of certain enzymes has garnered significant attention within the pharmaceutical industry for generating isotopically labelled chiral centres. While $NAD^+$-dependent reductases are already used in the asymmetric synthesis of pharmaceuticals, their use in deuterium labelling is constrained by the requirement for expensive isotopically labelled cofactors, such as 4-$d_1$-NADH ($d_1$-**51**), which must be regenerated *in situ* using $d_6$-ethanol, $d_8$-isopropanol, $d_{12}$-glucose, or $d_1$-formate. Recent work by Rowbotham *et al.* proposes an innovative method using $D_2O$ as the deuterium source in conjunction with a heterogeneous biocatalyst composed of a hydrogenase and an $NAD^+$-dependent reductase, with $H_2$ serving as the stoichiometric reductant and $D_2O$ as the deuterium donor (Scheme 6). This novel approach could mark the beginning of cost-effective enzymatic isotopic labelling in asymmetric synthetic chemistry, offering a promising alternative to traditional methods reliant on expensive cofactors.[19]

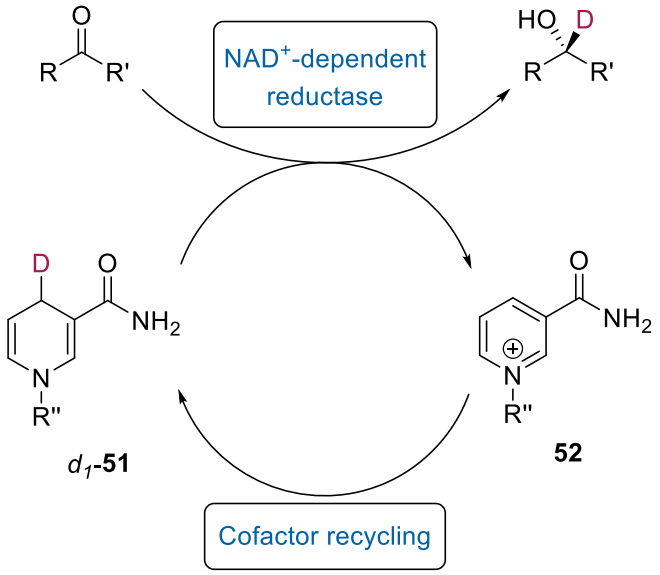


Scheme 6 General synthetic approach for the asymmetric deuteration using a $NAD^+$-dependent reductase.[19]

### 3.2.2. Transition Metal catalysed reductive Deuteration *via* $D_2$

The presence of unsaturated C–C bonds in naturally occurring compounds, pharmaceuticals, and industrial synthons makes these molecules highly suitable for deuterium incorporation through metal-catalysed reduction processes. Deuteration and hydro-deuteration, utilizing HD gas instead of $D_2$, can be achieved with transition metal catalysts in both heterogeneous and homogeneous systems. The commonly employed transition metals include iridium, rhodium, ruthenium, nickel, iron, copper or palladium. This methodology does not require the pre-incorporation of deuterium into the substrates. However, potential limitations include the use of a vast excess of highly flammable gases, as well as challenges in achieving precise chemo- and regioselectivity. (Scheme 7) [20,21]

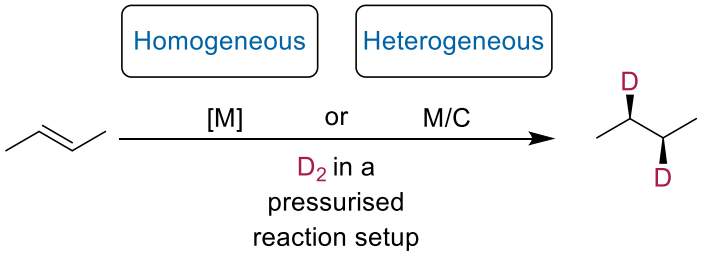


Scheme 7 General synthetic scheme of a homogeneous and a heterogeneous method for the deuteration of an alkene with $D_2$ as a deuterium source. [M] describes the transition metal M in the form of a complex. M/C describes the transition metal M on a carbon surface.[20,21]

### 3.2.3. Transition Metal catalysed reductive Deuteration using other Deuterium Sources

Deuterium incorporation into a molecule is frequently achieved via reduction strategies. Apart from the use of deuterium gas, deuterated equivalents of commonly employed hydride sources can be used. Depending on the starting material, commonly employed reagents include lithium aluminium deuteride (LAD, 10 € per mmol, abcr GmbH Oct. 2024), sodium borodeuteride ($NaBD_4$, 4 € per mmol, Merck Oct. 2024) or lithium borodeuteride ($LiBD_4$, 34 € per mmol, Merck Oct. 2024). However, these reactions have

a major limitation, as expensive deuterated reducing agents are required in equimolar quantities, and even in excess in the case of $NaBD_4$ as only one deuterium atom is incorporated in the final product. Asymmetric approaches with $LiAlH_4$ and chiral complexes (e.g. TADDOLs) have been reported with ees up to 96 % in ketone reductions.[22]

An alternative strategy involves the use of a catalytic system along with a more economical deuterium source to facilitate the reduction and incorporation of deuterium into the target compound. One approach of this type is the use of Noyori-type catalysts such as (*R,R*)- or (*S,S*)-RuCl[*p*-cymene)Ts-DPEN] [(*R,R*)- and (*S,S*)-**49**] in combination with deuterated formic acid (*d*$_1$-**50**) as the deuterium donor (4 € per mmol, euroisotope Nov. 2024). This catalytic methodology reduces the dependency on high amounts of costly reagents (such as $LiAlD_4$), potentially making the process more efficient and economically feasible as only 1.5 molar equivalents of *d*$_1$-**50** are needed as proven by Dinhof *et al.*.[18] Furthermore, Noyori-type catalysts (*R,R*)-**50** and (*S,S*)-**50** are known for their high stereoselectivity, allowing compounds to form with high enantiopurity. The Noyori-type catalyst offers additional advantages: the reaction is less sensitive to moisture or atmospheric oxygen than complex metal hydrides, reducing the need for strictly anhydrous or inert conditions. This enhances the practicality and efficiency of the reaction, making this method an appealing alternative for deuteration processes.[18,20]

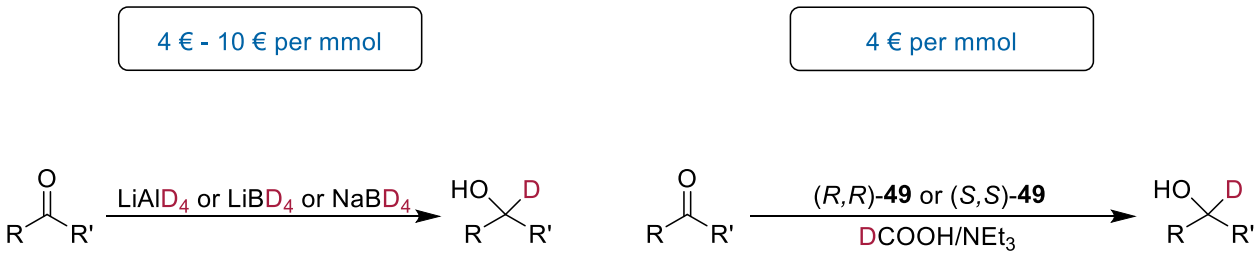


Scheme 8 Exemplified synthetic strategies for the incorporation of deuterium into a ketone *via* common reducing agents and their prices per mmol of Deuterium incorporated.

### 3.2.4. Corey-Seebach Umpolung and $D_2O$ as a Deuterium Source

The use of costly deuterated synthons, metal catalysts, or deuterium gas imposes significant limitations on the scalability of many of the above discussed deuteration reactions. Deuterium oxide would thus represent a more cost-effective and easily manageable alternative deuterium source. It can be used in a Corey–Seebach Umpolung strategy to achieve incorporation of deuterium into a target molecule, starting from an aldehyde. The formed dithiane is subjected to a subsequent deprotonation at C1- using a strong base, followed by the addition of $D_2O$ as the deuterium source. The aldehyde which is obtained after deprotection can be further used as a deuterated synthon for further reactions e.g. reduction with cheaper, non-deuterated (stereoselective) reagents (Scheme 9).[23]

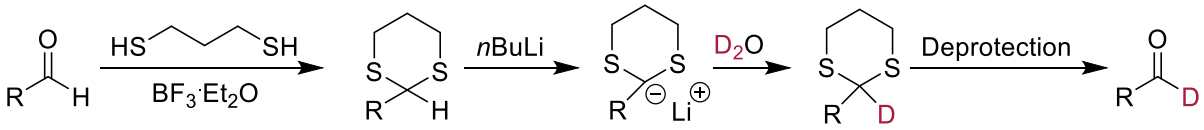


Scheme 9 Exemplified Corey-Seebach-Umpolung to yield a deuterated aldehyde as a powerful synthon for further synthesis.

## 3.3. Determination of the Absolute Configuration of Enantioisotopomers

Enantioisotopomers, in which a deuterium atom replaces a protium atom of a $CH_2$ group, are classified as enantiomers when the two other attached substituents differ. Consequently, accurate methods are required to assess their enantiomeric excess. This study employed a combination of either chiral solvating agents (CSAs) or derivatization strategies combined with nuclear magnetic resonance (NMR) spectroscopy as the method of choice on an everyday basis. This technique has been widely used in organic chemistry for many years, though it is now frequently superseded by chiral high-performance liquid chromatography (HPLC) for the determination of enantiomeric purities

of other types of enantiomers. However, due to the minimal structural differences between enantiomers that differ only by the substitution of a proton with deuterium, chromatographic methods often struggle to achieve sufficient resolution. In contrast, CSAs are sometimes able to reveal detectable differences, even in cases of minimal variations such as isotopic substitution or differences in alkyl chain length. The discriminatory ability of CSAs arises from the differential alignment of the two diastereomeric complexes formed between the enantioisotopomers and the CSA. However, the selection of effective CSAs is not governed by clear predictive rules and remains poorly understood. Furthermore, the selectivity of CSAs towards specific functional groups and the limited comparative data on different agents are significant drawbacks of this method. Two different CSAs (**57** and **58**) were tested and compared during this study. (Figure 6) [16,24,25]

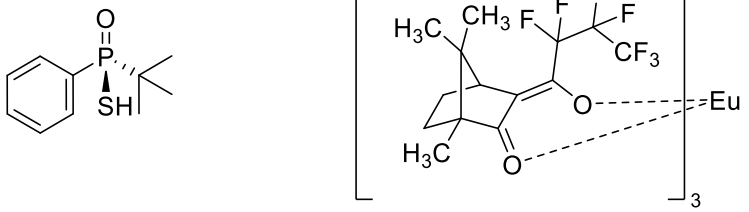


**53** **54**

Figure 6. Chemical structure of the CSAs (*S*)-*tert*-butyl(phenyl)-phosphinothioic acid (**53**) and Europium-tris[3-(heptafluorpropyl-hydroxymethylen)-(+)-camphorate] (**54**) used in this work.

CSAs provide a practical and straightforward approach for the determination of the enantioisotopomeric or enantiomeric excess; however, without enantiopure standards, the reliable assignment of the absolute configuration remains challenging. To address this, Sonstrom *et al.* developed a novel method that eliminates the need for enantiopure standards by employing chiral-tagged molecular rotational resonance (MRR) spectroscopy, which may enable high-throughput applications. In this method, the analyte is derivatized with a chiral tag molecule through non-covalent interactions, creating diastereomers. This derivatization occurs directly within the pulsed jet expansion, avoiding

additional chemical steps. First, the spectrum of the analyte's racemic form complexed with the chiral tag is measured, providing a baseline for instrument calibration. Then, the enantiomerically pure tagged sample is analysed, where the relative signal intensities directly reflect the enantiomeric ratio in the sample. The experimental data must be compared with quantum chemical calculations to assign the absolute configuration. This allows accurate stereochemical assignments based on the comparison of computationally predicted and observed actually measured MRR spectra.[26]

## 3.4. Determination of the Kinetic Isotope Effect

Due to the mass difference between protium and deuterium, a significant change in reaction rates is sometimes observed when a protium atom is replaced by a deuterium atom. This phenomenon, known as the kinetic isotope effect (KIE), provides valuable insights into chemical and biochemical processes. The KIE is defined as the ratio of the rate constants for a reaction involving a protium-containing substrate ($k^H$) compared to a deuterium-labelled analogue ($k^D$):

$$KIE = \frac{k^H}{k^D}$$

When the affected reaction occurs directly at the deuterium-labelled carbon, it is referred to as a primary KIE. This effect arises from the lower zero-point energy of the vibrational frequency of the carbon-deuterium bond compared to that of the carbon-protium bond. Although the transition-state energy barrier is the same for both reactions, the activation energy ($E_a$) for breaking the carbon-protium bond is lower than that for the carbon-deuterium bond. The relationship between the reaction rate and activation energy is given by:

$$k \sim e^{\frac{-E_a}{RT}}$$

Thus, the KIE can be expressed as:

$$KIE = \frac{k^H}{k^D} = \frac{e^{\frac{-E_{a,H}}{RT}}}{e^{\frac{-E_{a,D}}{RT}}} = e^{\frac{-\Delta E_a}{RT}}$$

Here, $\Delta E_a$ represents the difference in activation energies between the reaction of the protium-containing and deuterium-containing substrate, with a typical value of $\Delta E_a \approx$ 1.2 kcal/mol, leading to a KIE of approximately 7. However, empirical studies may show higher KIE values due to quantum mechanical tunnelling, which allows protons to traverse the energy barrier during proton transfer. Conversely, smaller KIE values are possible, and a KIE of 1 occurs when the carbon-deuterium bond is not broken or when bond-breaking is not part of the rate-limiting step of the studied reaction. Stopped-flow techniques are commonly employed to measure the KIE experimentally.[27]

# 4. Results and Discussion

## 4.1. Synthesis of the DfmD Substrates

The synthesis of the DfmD substrates *d*$_3$-**17** and *d*$_6$-**17** (see Scheme 3), was successfully achieved using the devised synthetic strategy. Compound *d*$_3$-**17** was readily synthesized following a literature-known procedure for the synthesis of the respective all-protio compound. $CD_3I$ (3 molar equivalents) was used for the quaternization of the amine **24** instead of $CH_3I$ for this purpose.[28] In contrast, the synthesis of *d*$_6$-**17** from **25** resulted in a mixture of mono-methylated, dimethylated, and trimethylated products. Various solvent systems (dry methanol, dry $Et_2O$, acetone) were studied to shift the reaction equilibrium toward the desired trimethylated compound *d*$_6$-**17**. However, neither changes in the solvent system nor an excess of methylating agent (max. 10 molar equivalents of $CD_3I$) did improve the yield. Typically, an equilibrium state was observed (48% trimethylated compound, 42 % dimethylated compound, 10 % monomethylated compound). Thus, the isolated yield could be improved by using Acetone as a solvent and removal of the desired, crystallised compound from the reaction mixture. After the removal of the product by filtration, the same equilibrium state was reached after 1 h. The crystalline solid was separated, followed by purification using IEC to give *d*$_6$-**17** as white solid.

The attempted synthesis of the unsaturated DfmD substrates *d*$_3$-**18** and *d*$_6$-**18** outlined in Scheme 4 was unsuccessful, primarily due to the failure of the planned Arbuzov reaction which did not lead to product formation due to unknown reasons. Consequently, an alternative synthetic route, inspired by a literature known synthetic route, was employed. Here, the desired unsaturated product should have been formed *via* compound **32** and subsequent methylation (Scheme 10. Attempted preparation of compound **57** via compound **56** using either *d*$_3$-methyl iodide and *d*$_3$-methyl triflate.).[29]

The synthesis of the unsaturated dimethylated compound **56**, synthesised *via* deprotonation of compound **55** and subsequent reaction with DMF in THF, was achieved with yields ranging from 24% to 30%. However, attempts to further methylate **56** using

methyl iodide were unsuccessful. Methyl triflate, synthesized following a literature protocol[30], was thus studied as an alternative, more reactive methylating reagent. Although trace amounts of the desired trimethylated product (compound **57**) were detected in the crude reaction mixture via ESI-MS, the product decomposed during the aqueous workup which caused the pH to drop to approximately 1. To mitigate this, 1 M sodium hydroxide was added to maintain the pH between 6 and 9 during the workup. Still, the product could not be isolated successfully.

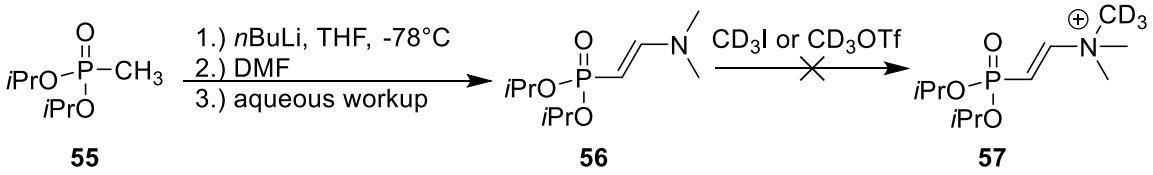


Scheme 10. Attempted preparation of compound **57** via compound **56** using either $d_3$-methyl iodide and $d_3$-methyl triflate.

An alternative approach could involve saturating the double bond of **56** *via* bromination with $Br_2$, followed by methylation using either methyl iodide or methyl triflate, and subsequently regenerating the double bond by DMSO mediated elimination of HBr (Scheme 11).[31] While ethyl and methyl protecting groups on the phosphonate moiety may be prone to hydrolysis under these conditions, the use of isopropyl groups might be beneficial to give the desired product $d_3$-**18**. Alternatively, different leaving groups at the C-1 position could be used to promote elimination and facilitate the formation of the desired double bond from a trimethylated, saturated intermediate. In order to obtain $d_6$-**18**, $d_6$-DMF could be used as starting material to give $d_3$-**60** as intermediate.

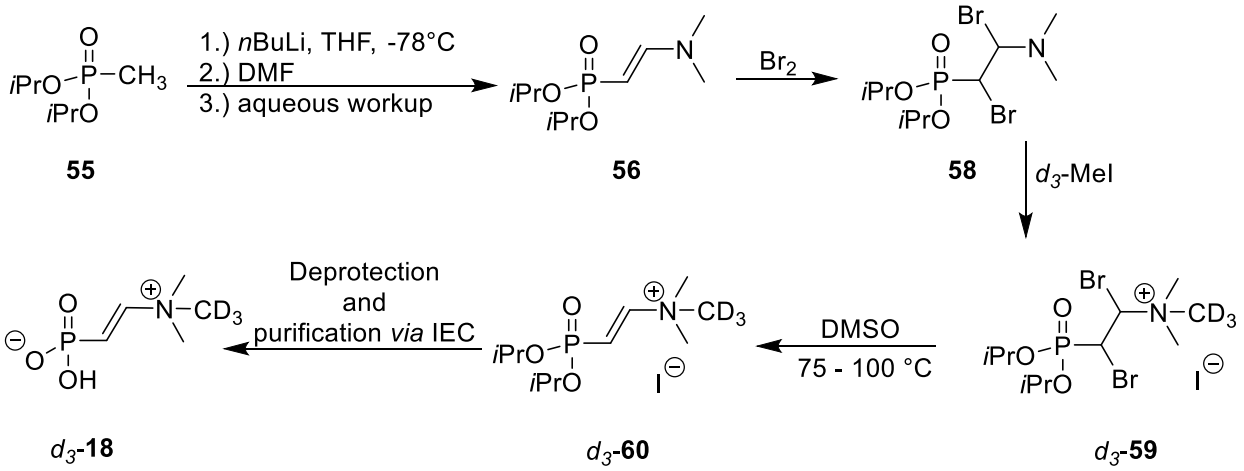


Scheme 11 Proposed alternative approach for the synthesis of compound $d_3$-**18**.

## 4.2. Synthesis of the FfnD and TmpA Substrates

The proposed synthetic steps to access compounds (*R*)-1-$d_1$-**19,** (*S*)-1-$d_1$-**19,** (*R*)-1-$d_1$-**20,** (*S*)-1-$d_1$-**20,** (*R*)-2-$d_1$-**20,** and (*S*)-2-$d_1$-**20** were tested using un-deuterated compounds and all of them could be successfully performed and the yield optimised. The reduction of aldehydes **37, 38** and **39** to form the primary alcohols **40**, **41**, **42** was successfully achieved using (*S,S*)-**49** *and* (*R,R*)-**49** in combination with HCOOH/$Et_3N$ as the hydride source (Scheme 5).

The different Apple-type reactions were successfully carried out for all compounds, testing two different bromine donors: carbon tetrabromide ($CBr_4$) and *N*-bromosuccinimide (NBS). The reaction with $CBr_4$ as the bromine donor proceeded smoothly at 0°C without protection from sunlight. In contrast, the NBS-mediated reaction required more stringent conditions (performed at −78°C and in complete darkness) to prevent radical formation and the resulting side products. Both methods achieved high yields (>90%), but due to the simpler handling and milder conditions required, the $CBr_4$-based reaction was chosen as the preferred method for all compounds.[17,32] Like this, the brominated intermediates **43, 44** and **45** could be successfully obtained. **43** and **44** were then subjected to an Arbuzov reaction to give phosphonates **46** and **47** in yields above 60 %, respectively after 18 h at 160°C**.**

By performing a Williamson ether synthesis by reacting bromide **45** with potassium phthalimide, **46** was equally accessible, as needed for the incorporation of deuterium at C2.[28]

A naphthyl protecting group was first envisaged for the synthesis of the FfnD substrates (*R*)- and (*S*)-1-$d_1$-**19**, to facilitate the detection of the intermediates by UV-detectors. To improve the atom economy of the process, the naphthyl protecting group was however replaced with a benzyl group, which behaved similarly in all studies reactions.

The performed asymmetric transfer deuteration (ATD) could be successfully performed to incorporate one deuterium atom during the reduction of the three key aldehydes. However, NMR spectroscopic analysis of the mono-deuterated products using the CSAs [(*S*)-*tert*-butyl(phenyl)phosphinothioic acid (**53**) and **54**] indicated unsatisfactory results regarding enantioisotopomeric excess, as no distinguishable chemical shift was observed for any signal of the prepared racemic samples of compounds *rac*-$d_1$-**40**, *rac*-$d_1$-**41** and *rac*-$d_1$-**42** using **54. 54** resulted in very broad peaks in the NMR spectra due to the long relaxation time associated with Europium, complicating resolution and interpretation; thus, whenever a phosphonate is studied and thus **53** can be used, it should be favoured. Formation of a Mosher ester of compound (*R*)-$d_1$-**40** and (*S*)-$d_1$-**40** also provided inconclusive results. Consequently, it remains uncertain whether a racemic mixture was synthesized, leaving the stereoisomeric composition of the deuterated key alcohols (*R*)-$d_1$- and (*S*)-$d_1$-**40** undetermined.

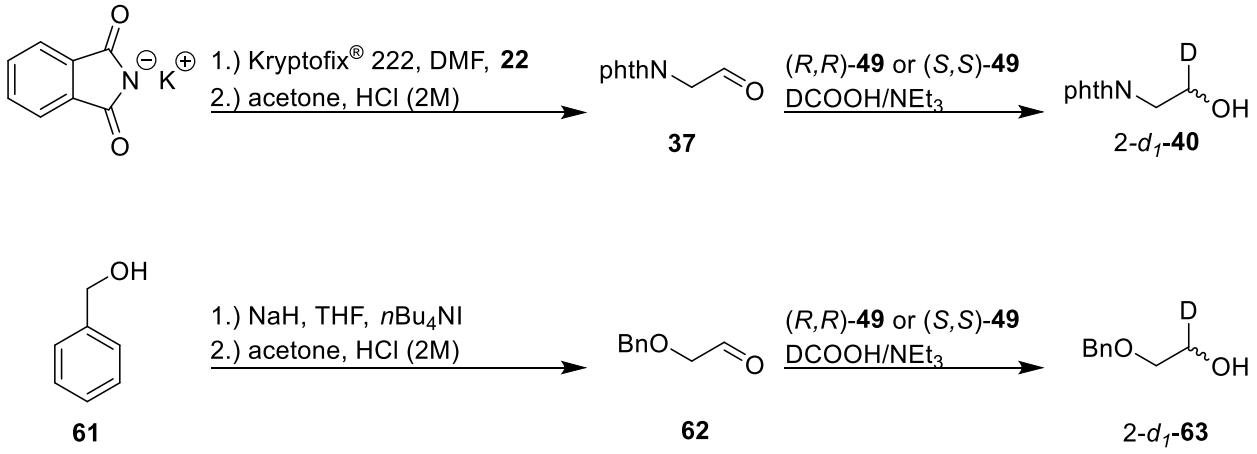


Scheme 12 Deuterated key alcohols (*R*)-, (S)-2-$d_1$-**40** and (R)-, (S)-1-$d_1$-**63** with undetermined enantioisotopomeric excess.

While the ee of (*R*)-$d_1$-**42** and (*S*)-$d_1$-**42** could not be determined using CSA **54**, the use of CSA **53** allowed for an approximate determination of the ee of 18 %. The broadened td belonging to the remaining C-1 proton, next to the phosphorus showed a measurable signal splitting upon addition of **53** to the NMR sample.

Thus, unfortunately the planned asymmetric transfer deuteration (ATD) needed to be replaced by a different stereoselective reduction method. In theory, this equally applies to the synthesis of the planned C-1 and C-2 deuterated compounds. However, as the determination of ee proved to be very difficult for alcohols (*R*)-*d*$_1$-**40**, (*S*)-*d*$_1$-**40,** (*R*)-*d*$_1$-**41**, (*S*)-*d*$_1$-**41,** (*R*)-*d*$_1$-**42** and (*S*)-*d*$_1$-**42**, the focus of this section of the thesis was shifted towards the synthesis of mono-deuterated primary alcohols derived from diethyl 2-oxoethylphosphonate (**39**). Although asymmetric reduction using a deuteride and a chiral catalyst was considered as a potential approach, the use of a deuterated aldehyde in combination with varied hydride sources and catalysts was not chosen in the first place as the more cost-effective strategy. The original pathway offers a more efficient route to achieve the desired deuteration while maintaining cost-effectiveness in the synthesis. Since no literature methods are available for determining the enantioisotopomeric excess of the naphthyl- or phthalimide-protected compounds [(*R*)- and (*S*)-*d*$_1$-**40** (*R*)- and (*S*)-*d*$_1$-**41**], we first aimed for the synthesis of (*R*)- and (*S*)-*d*$_1$-**42**, as their absolute configurations can be assigned after Mosher esterification .[16] Consequently, the synthesis of the deuterated phosphonoacetaldehyde derivative *d*$_1$-**39** was prioritized. The respective non-deuterated aldehyde **39** was synthesised *via* an Arbuzov reaction of bromoacetaldehyde diethyl acetal (**64**) with triethyl phosphite, followed by deprotection of the acetal group. The synthesis of the deuterated aldehyde *d*$_1$-**39** was first attempted by a 7-step synthesis reported by Wang *et al.* which was not reproducible due to complete degradation of the product in the final step. However, the synthesis of aldehyde *d*$_1$-**39** was successfully achieved in 75% yield by deprotonation of diethyl methyl phosphonate in the presence of *n*-BuLi followed by addition of *d*$_7$-DMF and an aqueous hydrolysis of the formed enamine. (Scheme 13) [29,33]

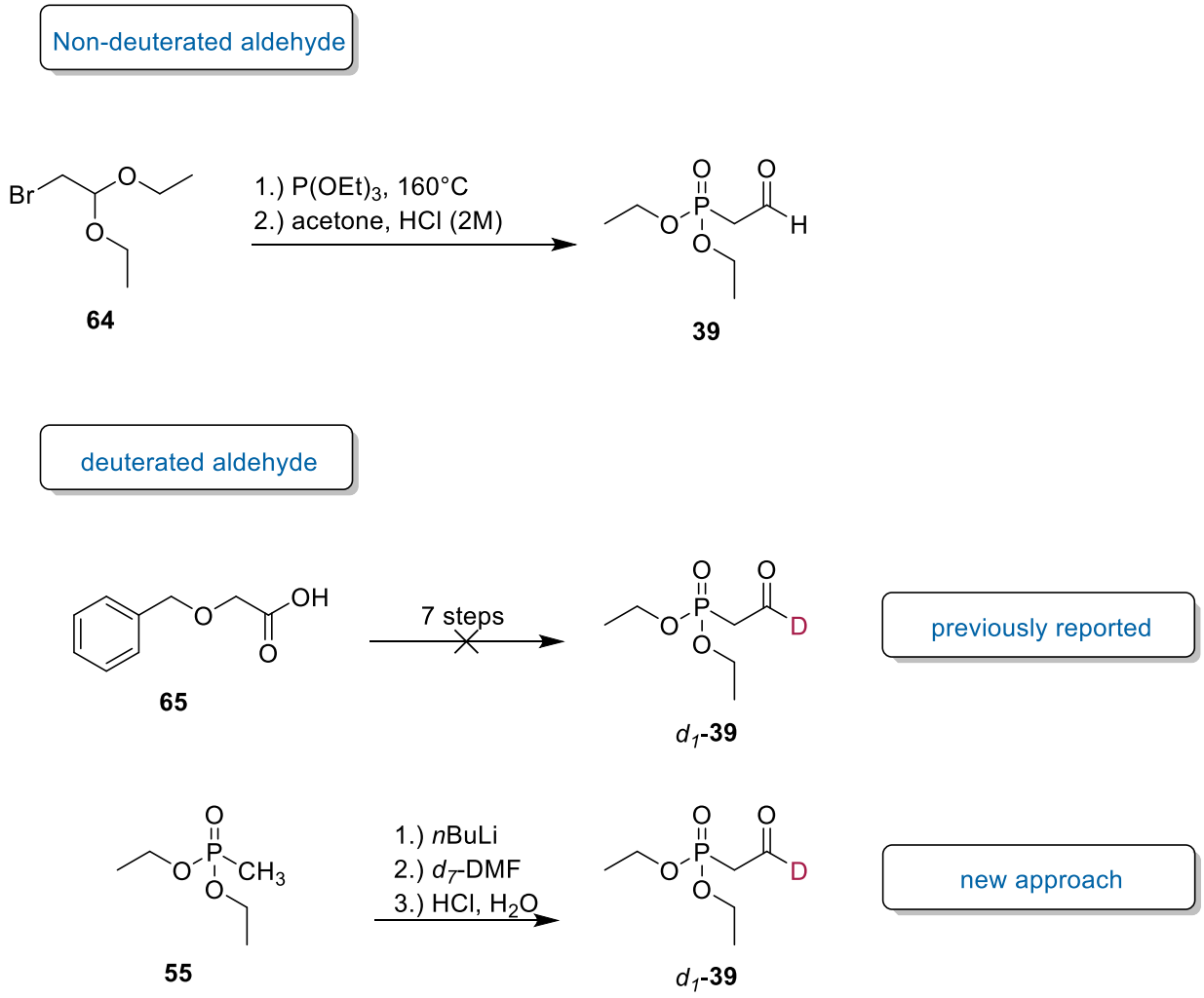


Scheme 13 Synthesis of the non-deuterated and the deuterated key aldehyde.

With the deuterated aldehyde in hands, three different catalytic reductions were tested: (*R*)-1-Methyl-3,3-diphenylhexahydropyrrolo[1,2-c][1,3,2]oxazaborole (CBS) catalyst with catecholborane[34] or borane dimethyl sulfide as stoichiometric reductants and (*R*)-Alpine borane®.[33] The enantioisotopic excess was estimated in all cases by adding (*S*)-*tert*-butyl(phenyl)-phosphinothioic acid (**53**) as a CSA to an NMR sample of the obtained alcohol. This method could however not provide results of the same accuracy as were found by NMR analysis of the formed Mosher ester. (Scheme 14)

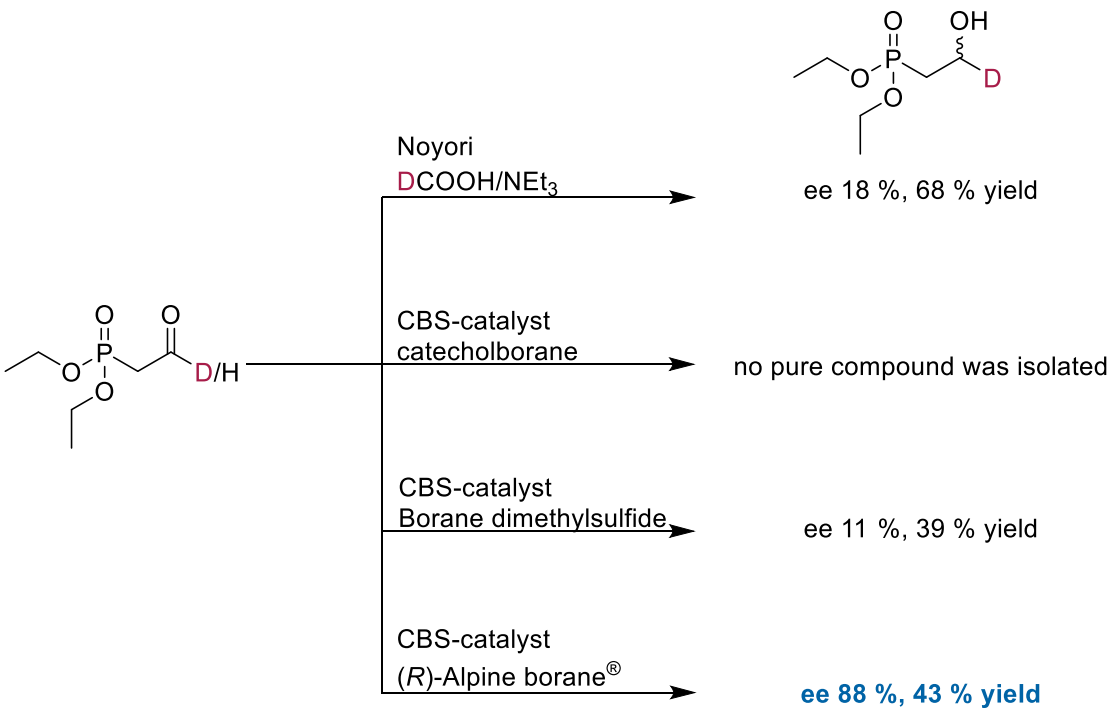


Scheme 14 Overview of the different reduction methods.

In conclusion, the (*R*)-Alpine borane® -mediated reduction appears to be by far the most promising approach (ee 88 %) for synthesizing all target compounds. Like this, both enantiomers of compounds (*R*)-$d_1$-**42** and (*S*)-$d_1$-**42** deuterated at the C-2 position are accessible using the developed synthetic pathway. However, challenges remain for the synthesis of the compounds deuterated at the C-1 position, as benzyl- or naphthyl-protected methanol cannot be reacted with $d_7$-DMF in the same way due to a low stability when exposed to organolithium bases and a lack of acidic protons to abstract.

An alternative strategy involving a Corey–Seebach Umpolung approach to generate the desired deuterated aldehydes $d_1$-**37** and $d_1$-**38** which could be reduced using varied conditions might facilitate access to the corresponding alcohols (*R*)- and (*S*)-$d_1$-**40** and (*R*)- and (*S*)-$d_1$-**41**, thereby enabling the synthesis of all target products. However, due to time constraints, only one test reaction using the dithiane derived from aldehyde **37** could be performed. Unfortunately, the desired product was not detected in the complex reaction mixture due to possible decomposition of the phthalimide moiety.

## 4.3. Stopped-flow Measurements and Enzymatic Assays of (*S*)-1-$d_1$-**19**, **19**, $d_3$-**17** and **17**

### 4.3.1. Deuterated and non-deuterated FfnD Substrates (*S*)-1-$d_1$-**19** and **19**

With target compounds (*S*)-1-$d_1$-**19** and **19** in hands, triple quadrupole mass spectrometry assays were performed to study FfnD. Turnover is occurring with the protium-labelled substrate (**19**) but not with the deuterated compound (*S*)-1-$d_1$-**19**. The production of succinate across all conditions indicates that the enzyme retains some level of activity. This partial activity suggests that the enzyme may be undergoing catalysis but is not effectively coupling with the deuterated substrates, possibly due to a KIE impacting specific steps in the reaction mechanism. This reduced coupling efficiency with the deuterated substrates might reflect a rate-limiting step sensitive to isotope substitution, impeding the enzyme's full catalytic cycle with these substrates. Further analysis, such as examining intermediate formation rates or altering assay conditions, could help determine if the coupling inefficiency is due to intrinsic isotope effects or structural alterations in enzyme-substrate interaction.

During the stopped-flow analysis, it was observed that the enzyme shows delayed activity, characterized by an extended mixing phase before the ferryl-intermediate forms (Figure 7). This prolonged phase raised the question of whether the observed delay is a true kinetic feature of the enzyme or an artifact stemming from suboptimal assay conditions, such as mixing inefficiencies or pH fluctuations. Once the ferryl formation initiates, the phase appears consistent and smooth, with no interruptions or irregularities. Additionally, evidence of a KIE suggests that the rate-determining step may involve a bond that is sensitive to isotopic substitution, supporting the idea that ferryl formation and subsequent turnover are genuine rather than artifacts. Further controls to refine the assay conditions, like improving mixing efficiency or adjusting buffer composition, could clarify whether this initial delay is intrinsic, or artifact related.

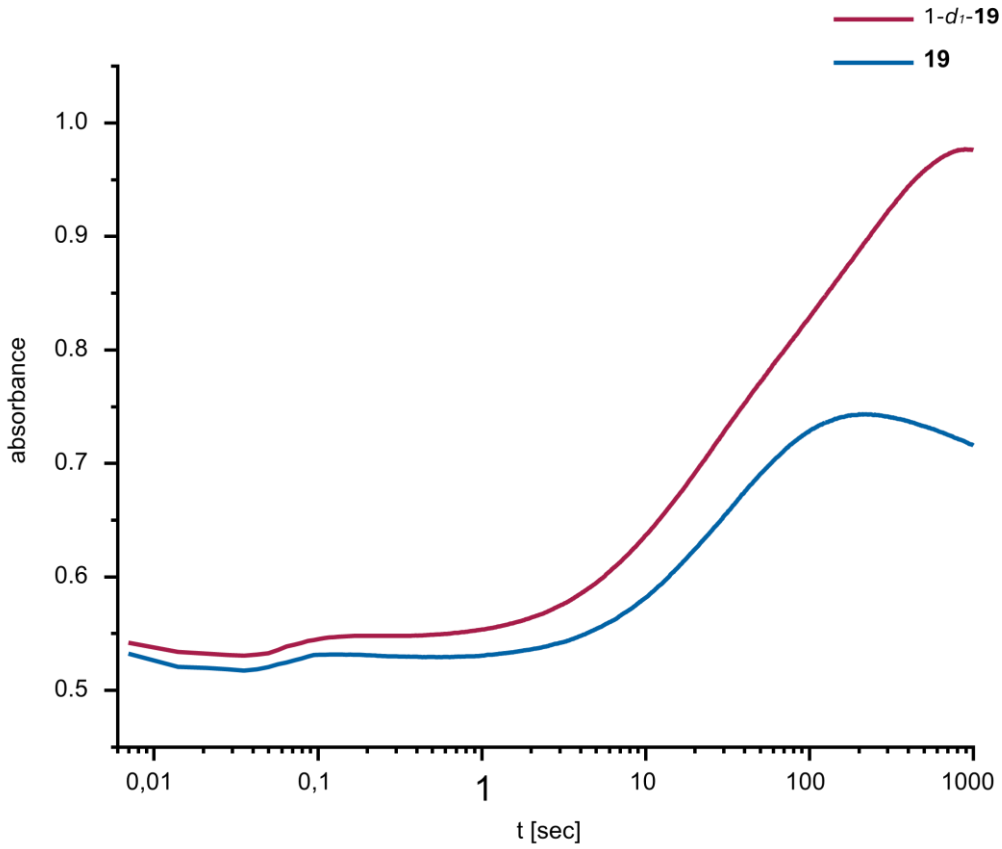


Figure 7 Stopped-flow measurements of the FfnD Substrates 1-$d_1$-**19** and **19**.

Based on the performed $^{31}$P NMR assay, it appears that the enzyme shows only marginal activity with the protium-labelled substrate (**19**) and lacks activity altogether with the deuterated compound (*S*)-1-$d_1$-**19** (Figure 8). This inactivity could stem from substantial uncoupling of the enzyme, potentially due to improper protein folding or anomalies in metalation that impair the active site's function. Misfolding might affect substrate binding and alignment within the active site, while faulty metal incorporation could disrupt catalytic turnover. Further analyses, such as assessing the enzyme's secondary structure (e.g., CD spectroscopy) or confirming metal cofactor integrity (e.g., ICP-MS or EPR spectroscopy), might help identify whether these factors are causing the observed catalytic inefficiency.

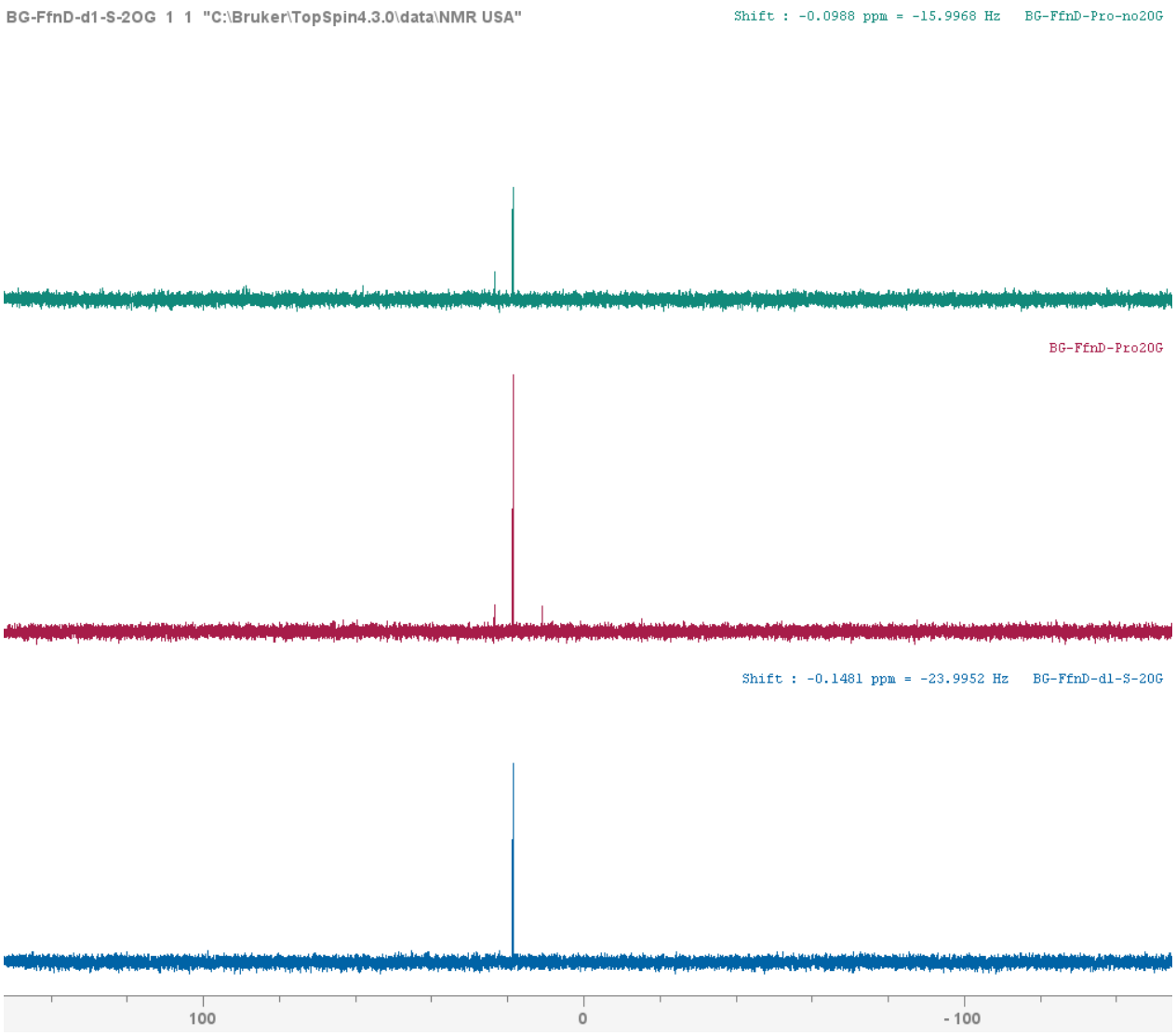


Figure 8 $^{31}$P NMR assay of FfnD Substrates **19** (red) and (*S*)-1-$d_1$-**19** (blue) in comparison to **19** without 2OG (green).

The discrepancy in turnover between the protium and deuterated substrates, where only the protium-labelled substrate demonstrates any activity, further supports the hypothesis of an influence of a KIE. This may be causing a rate-limiting step in the catalytic cycle, as the deuterium substitution likely affects bond dissociation energies at critical points in the reaction. To clarify these observations, optimizing assay conditions (e.g., mixing, buffer composition) and performing structural analyses—such as CD spectroscopy for protein

folding and ICP-MS or EPR for metal content—could confirm whether these activity limitations are due to enzyme properties or assay artifacts.

### 4.3.2. Deuterated and non-deuterated DfmD Substrates *d*$_3$-**17** and **17**

The mass spectrometry analysis of the DfmD substrates *d*$_3$-**17** and **17** yielded significantly improved results. Products were clearly detectable for both substrates, and deuterium incorporation was observed at all three possible positions: the methyl group attached to nitrogen, the methylene group within the chain, and, in part, lost as formaldehyde (Scheme 2). This pattern of incorporation indicates successful labelling and suggests that deuterium transfer and retention are occurring, providing insights into substrate processing and potential reaction pathways.

In the DfmD stopped-flow analysis, the synthetic deuterated substrate exhibited behaviour nearly identical to the protium substrate, as observed in the mass spectrometry results (Figure 9). This similarity was anticipated under single-turnover conditions, where the enzyme does not interact with the methyl hydrogens, minimizing any observable isotope effect. In the multi-turnover regime, any effect on the substrate remains too subtle to definitively confirm, suggesting that if a kinetic isotope effect (KIE) is present, it is likely small and challenging to detect within the current assay setup.

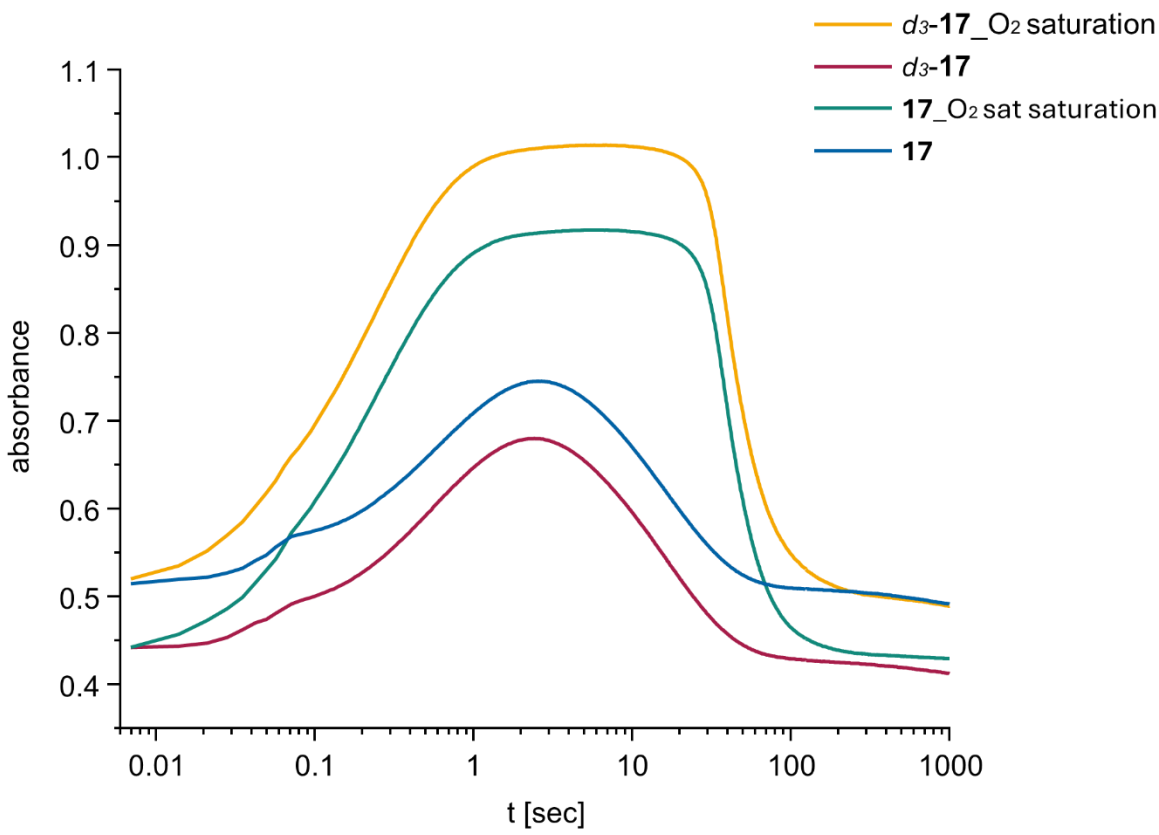


Figure 9 Stopped-flow measurements of the DfmD substrates *d*$_3$-**17** and **17** under single-turnover conditions and multiple-turnover conditions ($O_2$ saturation).

The $^{31}P$ NMR analysis of the DfmD substrates showed the presence of products for both the deuterated and protium substrates. The observed product ratios were consistent with those determined from the mass spectrometry data, further confirming the validity of the results across both methods.

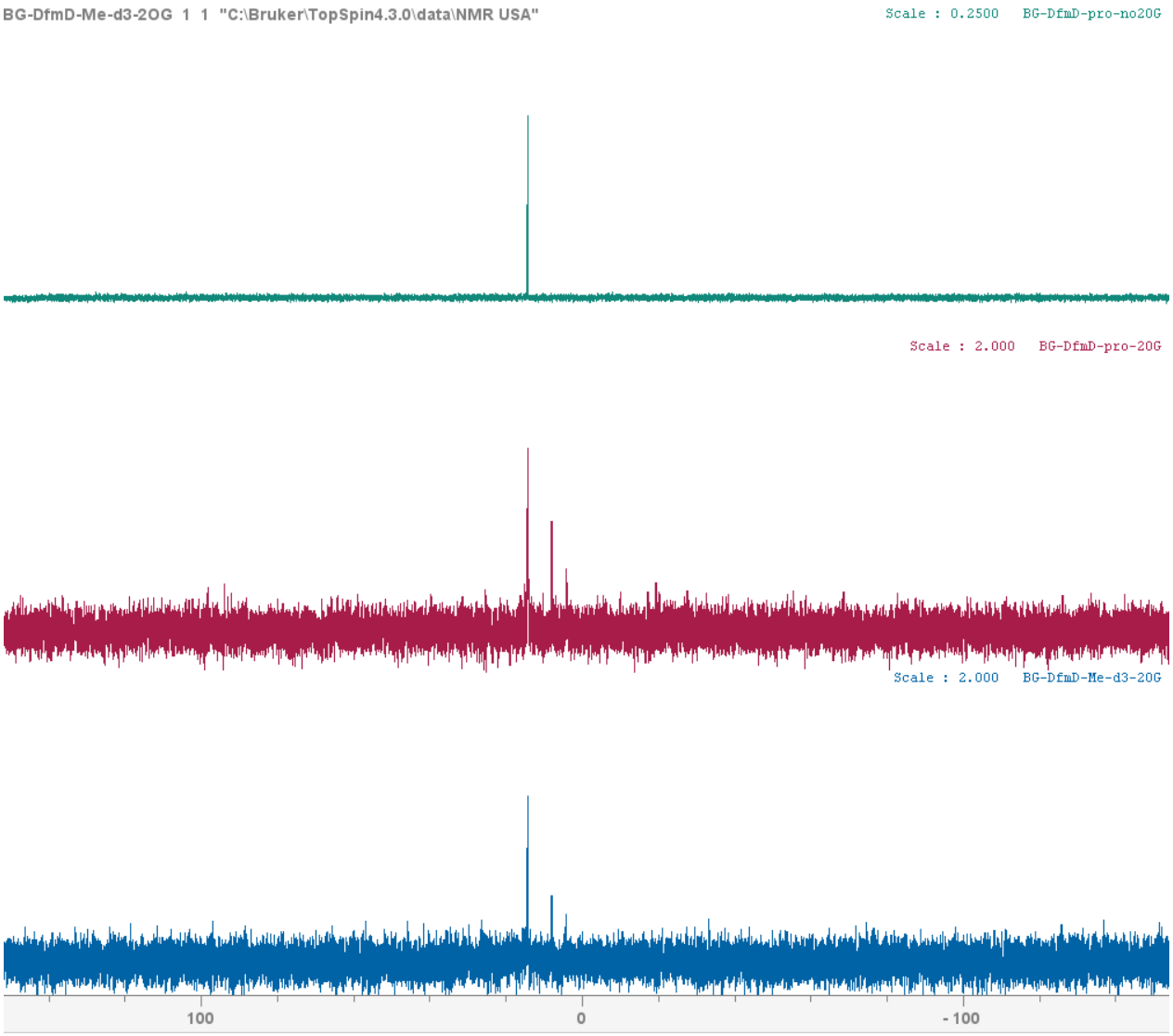


Figure 10 $^{31}$P NMR assay of DfmD Substrates 17 (red) and *d*$_3$-**17** (blue) in comparison to **17** without 2OG (green).

In conclusion, the kinetic and spectroscopic analysis of the DfmD and FfnD substrates provided insights into the enzymes' activities and substrate incorporation. Mass spectrometry revealed that deuterium was effectively incorporated at all three possible positions in the DfmD substrates, confirming successful labelling, although the synthetic deuterated substrate had similar characteristics to the protium substrate under single-turnover conditions. The $^{31}$P NMR analysis corroborated these findings for both DfmD and FfnD substrates, showing the expected products and confirming ratios consistent with

mass spectrometry results. However, in multi-turnover conditions, any observable kinetic isotope effect appeared too subtle to discern. Overall, the results highlight the enzymes' behaviour and substrate interactions while suggesting the need for further investigation to detect potential effects under different assay conditions.

# 5. Experimental Part

## 5.1. General Experimental Part

The used chemicals were obtained from abcr chemicals, Sigma-Aldrich, TCI, Fluka, Euroisotop or Acros.

Thin layer chromatography was conducted using Merck silica gel 60 $F_{254}$ plates, coated 0.25 mm thick. Visualisation of spots was performed using UV light and the below described stains as indicated for the respective compounds.

Table 1 Composition of the used TLC stains.

| | |
|---|---|
| Vanillin stain | 15 g vanillin in 250 mL ethanol and 2.5 mL $H_2SO_4$ (conc.) |
| CAM stain | 46 g $(NH_4)_6Mo_7O_{24}$ x 4 $H_2O$, 2 g $Ce(SO_4)_2$ x 4 $H_2O$ in 1 L 10% $H_2SO_4$ |
| $KMnO_4$ stain | 9 g $KMnO_4$, 60 g $K_2CO_3$ in 900 mL $H_2O$ and 15 mL 5% NaOH (aq.) |

Compound purification was performed by medium-pressure liquid chromatography (MPLC) using a Biotage Isolera Prime® flash purification system using either pre-packed Sfär-Duo separation cartridges or self-filled Sfär-Duo or KP-Sil cartridges in combination with Machery-Nagel silica gel 60 (230-400 mesh). Ion exchange chromatography (IEC) was performed using either Dowex 50W × 8/$H^+$-form as cation exchange system or Dowex Monosphere-550A/$OH^-$- form as anion exchange system.

NMR spectra were recorded either on a Bruker BioSpinAV III HD 700 ($^1$H: 700.40 MHz, $^{13}$C: 176.12 MHz), AV III 600 ($^1$H: 600.25 MHz, $^{13}$C: 150.93 MHz, $^{31}$P: 242.99 MHz), AV NEO 400 ($^1$H: 400.27 MHz, $^{31}$P: 162.03 MHz) or AV NEO NanoBay 400 ($^1$H: 400.13 MHz, $^{31}$P: 161.98 MHz) spectrometer and the recorded spectra were referenced as in Table 2.

Table 2 Solvent (residual) signals used for calibration of the recorded NMR spectra.

| Nucleus | Solvent | referenced to | Shift / ppm |
|---|---|---|---|
| $^{1}H$ | $CDCl_3$ | $C\mathbf{H}Cl_3$ | 7.26 |
| | $D_2O$ | **H**OD | 4.79 |
| | Toluene-$d_8$ | $(C_6D_5)C\mathbf{H}D_2$ | 2.08 |
| | Methanol-$d_4$ | $C\mathbf{H}D_2OD$ | 3.31 |
| $^{13}C$ | $CDCl_3$ | $\mathbf{C}DCl_3$ | 77.16 |
| | Methanol-*d4* | $\mathbf{C}D_3OD$ | 49.00 |
| $^{31}P$ | External $H_3PO_4$ | $H_3\mathbf{P}O_4$ | 0.00 |

Mass spectra were recorded on either a UltiMate 3000 RSLCnano system – capillary flow (Thermo Scientific) or a Ultimate 3000 HPLC system (Thermo Scientific) coupled with Bruker maXis UHR-TOF *via* electrospray ionization (ESI).

Stopped-flow UV/VIS absorption spectroscopy (stopped-flow) experiments were carried out at 5 °C using an Applied Photophysics Ltd. (Leatherhead, UK) SX20 instrument housed in an anoxic chamber (Labmaster, MBraun, Stratham, MA, USA). The instrument was configured for single mixing with an optical path length of 1 cm, and the data was acquired using both a photodiode array (PDA) and a photomultiplier tube (PMT) detector.

Liquid chromatography coupled to mass spectrometry (LC–MS) was carried out on a 1200 series LC system connected to a 6410 triple quadrupole mass spectrometer (Agilent Technologies).

## 5.2. Synthesis of $d_1$-Formic Acid ($d_1$-**50**)

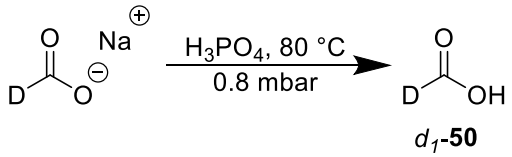


$d_1$-**50**

Deuterated sodium formate (65.5 mmol, 4.51 g, 1 eq.) was combined with orthophosphoric acid (393.5 mmol, 39.86 g, 6 eq.) and melted under an argon atmosphere at 50°C. Once the melting process is nearly complete, the product was distilled over a vacuum distillation bridge at 80°C (0.8 mbar) into a Schlenk flask maintained at −196°C. The process yielded $d_1$-formic acid ($d_1$-**50**) as a viscous, colourless liquid in quantitative yield.[35]

**$^1$H NMR** (400.27 MHz, $D_2O$, [42May2124/300]): $\delta_H$ = 8.16 (s, C(O)OH).

**$^{13}$C NMR** (100.65 MHz, $D_2O$, [42May2124/302]): $\delta_C$ = 166.18 (t, C(O)OH).

## 5.3. General Procedures

### 5.3.1. General Procedure I: Synthesis of diethoxy Compounds from bromo acetaldehyde diethyl acetal

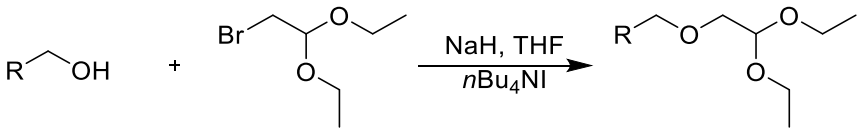


NaH (1.8 eq.) is suspended in THF (0.5 mL/mmol) under argon. The suspension is cooled to 0°C and vigorously stirred. After the addition of *n*Bu$_4$NI (0.01 eq.), suspended in THF (2 mL/mmol), the respective alcohol (1.0 eq.) is added slowly in portions and the resulting suspension is stirred for 30 minutes at 0°C. Afterwards, bromo acetaldehyde diethyl acetal (**64**, 1.0 eq.) is added and the reaction mixture is heated to 60°C and stirred for the indicated time (monitored by TLC). After completion, the reaction mixture is poured

on ice. The phases are separated, and the aqueous phase is extracted three times with DCM. The organic phases are combined, dried ($Na_2SO_4$), filtered and reduced *in vacuo*. The crude product is purified by MPLC using the indicated solvent gradient.

### 5.3.2. General Procedure II: Aldehyde Synthesis *via* acidic Hydrolysis of the diethyl acetals

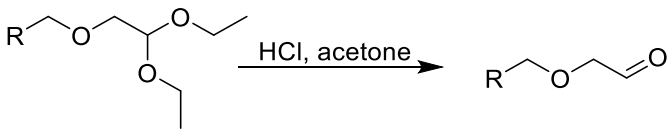


The respective diethyl acetal is dissolved in acetone (2 mL/ mmol). Afterwards, aqueous HCl (2 M, 3 mL/mmol) is added, and the solution is stirred until completion of the reaction. Saturated aq. $NaHCO_3$ is added, the phases are separated, and the aqueous phase is extracted 3 times with DCM. The combined organic phases are dried ($Na_2SO_4$), filtered and the solvent is removed *in vacuo*. The product is either purified *via* MPLC using the given solvent gradient or by distillation as indicated.

.

### 5.3.3. General Procedure III: Synthesis of primary Alcohols *via* Catalytic Transfer Hydrogenation.

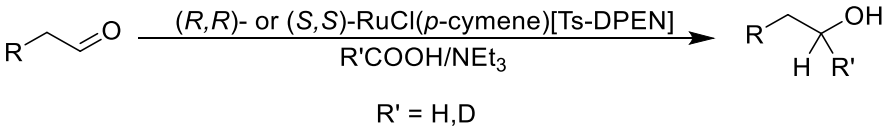


R' = H,D

***Activation of the catalyst***

(*R,R*)- or (*S,S*)-RuCl(*p*-cymene)[Ts-DPEN] [(*R,R*)-**49** or (*S,S*)-**49**], is dissolved in dry DCM (1 mL/40 mg of catalyst) and an aqueous KOH solution (0.2 M, 1 eq.) and water (0.3 mL/40 mg of catalyst) are added. The biphasic mixture is vigorously stirred,

causing the solution to change its colour from orange to violet. The layers are separated using a syringe as a separation funnel. The aqueous layer is washed with DCM (3 × 0.5 mL), and the combined organic phases are carefully dried ($CaH_2$) and filtered over a cotton plug. The catalyst can be used as-is without further purification or stored in the freezer under Ar for approximately one month.[18]

***Asymmetric transfer Hydrogenation/Deuteration***

Formic acid (4.40 eq.) or $d_1$-formic acid ($d_1$-**50**, 4.40 eq.) is added dropwise to triethylamine (2.60 eq.) at 0°C under an argon atmosphere and the resulting mixture is stirred for 30 minutes. Meanwhile, the respective aldehyde (1.0 eq.) is dissolved in DCM (4 mL/mmol) under argon. The mixture of triethylamine and formic acid is then slowly added to the solution of the starting material. The activated catalyst [(*R,R*)- or (*S,S*)-**49,** 0.007 eq.] is added, and the reaction is stirred at 35°C under an inert atmosphere. The progress of the reaction is monitored by TLC. After completion, the solvent is removed *in vacuo* and the product purified *via* MPLC using the given solvent gradient.[18]

### 5.3.4. General Procedures IV A and B: Dehydroxy-Bromination Reaction of Alcohols *via* Appel-type Reactions

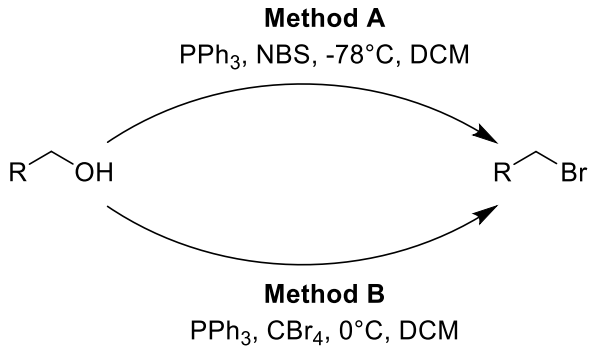


***Method A***

NBS (1.2 eq.) is added to DCM (3.5 mL/mmol of alcohol) at −78°C in the darkness and. $PPh_3$ (1.3 eq.) in DCM (2.5 mL /mmol) is added over a period of 20 minutes and the resulting mixture is stirred until it becomes a clear solution. The required alcohol is

dissolved in DCM (1.5 mL/mmol of alcohol) and slowly added to the NBS/$PPh_3$ solution. After stirring for 10 minutes at −78°C, the cooling bath is removed and the reaction is allowed to warm to room temperature. The progress of the reaction is monitored by TLC. After completion, the solvent is removed *in vacuo* and the product purified *via* MPLC as indicated for the respective compound.[17]

***Method B***

The respective alcohol (1 eq.) and $CBr_4$ (1.6 eq.) are dissolved in dry DCM (5 mL/mmol of alcohol) and cooled to 0°C under an argon atmosphere. After cooling, $PPh_3$ (1.5 eq.) is added, and the reaction is allowed to warm up to room temperature. The progress of the reaction is monitored by TLC. After completion, the solvent is removed *in vacuo* and the product is purified *via* MPLC as indicated.[32]

### 5.3.5. General Procedure V: Arbuzov Reaction of brominated Compounds

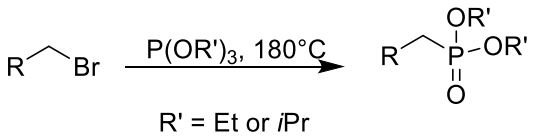


The respective bromide (1 eq.) is combined with the required trialkyl phosphite (10 eq.) and stirred at 180°C. The progress of the reaction is monitored by NMR. The product is purified *via* vacuum distillation or MPLC as indicated.

## 5.4. Synthesis of the FfnD and TmpA Substrates

### 5.4.1. Synthesis of Compound **35**

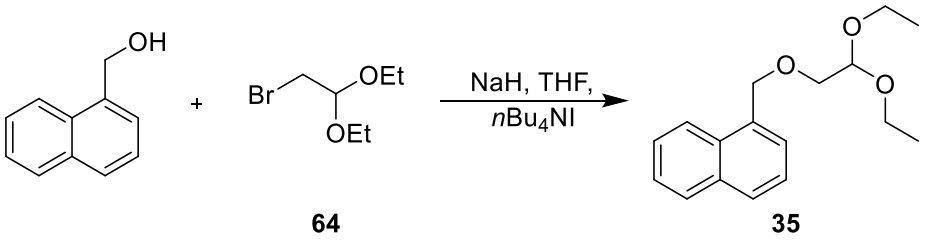


**64** **35**

The reaction of naphthalene-1-yl-methanol (3.082 g, 19.5 mmol, 2.0 eq.) and bromo acetaldehyde diethyl acetal (**64**) was performed according to **general procedure I** to give **35** (2.69 g, 9.81 mmol, quant.) as a clear, yellow oil after purification *via* MPLC. [$R_f$ (*n*-heptane:EtOAc = 3:2) = 0.37; gradient 8 % → 50 % EtOAc in *n*-heptane]

**$^1$H NMR** (400.27 MHz, $CDCl_3$, [42Apr2324/360]): $\delta_H$ 8.20 (1H, t, *J* = 4.6 Hz, arom), 7.90-7.82 (2H, m, arom), 7.58-7.49 (3H, m, arom), 7.45-7.40 (1H, m, arom), 5.06 (2H, s, $CH_2$ Bn), 4.70 (1H, t, *J* = 5.3 Hz, CH), 3.71 (4H, $ABX_3$, A-part: qd, $J_{AB}$ = 9.3 Hz, $J_{AX}$ = 7.1 Hz; B-part : $J_{AB}$ = 9.3 Hz, $J_{BX}$ = 7.1 Hz, 2 × $C\underline{H_2}$-$CH_3$), 3.61 (2H, d, *J*= 5.3 Hz, $CH_2$), 1.23 (6H, t, *J* = 7.1 Hz, 2 × $CH_3$).

**HRMS** calculated for $C_{17}H_{22}O_3$ (274.1568 g/mol): *m/z* 297.1467 $[M+Na]^+$; found: *m/z* 297.1461.

### 5.4.2. Synthesis of Compound **38**

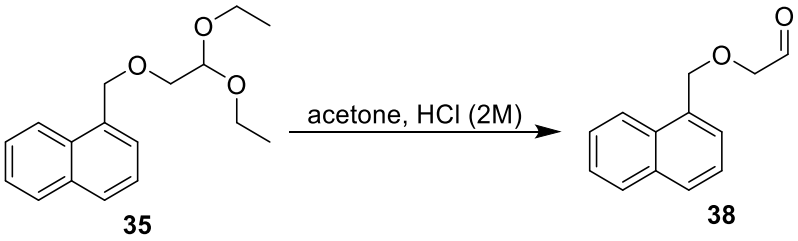


The synthesis of compound **38** (1.564 g, 7.81 mmol, 80%) was performed according to **general procedure II** starting from **35** (2.554 g, 9.81 mmol, 1 eq.). The crude residue was purified *via* MPLC [$R_f$ (n-heptane:EtOAc = 3:2) = 0.65; gradient 8 % → 95 % EtOAc in *n*-heptane] to give the desired product as a bright yellow liquid.

**$^1$H NMR** (400.27 MHz, $CDCl_3$ , [42May1524/340]): $\delta_H$ 9.69 (1H, symmetric m, C(O)H), 8.20 (1H, t, *J* = 4.6 Hz, CH arom), 7.90-7.82 (2H, m, CH arom), 7.58-7.49 (4H, m, CH arom), 7.45 (1H, q, *J* = 5.0 Hz, CH arom), 5.09 (2H, s, $CH_2$ Bn), 4.14 (2H, d, *J* = 0.7 Hz, $C\underline{H_2}$-C(O)H).

**$^{13}$C NMR** (100.65 MHz, $CDCl_3$, [42May1524/341]): $\delta_C$ 200.52 (1C, s, C(O)H), 133.92 (1C, s, quart. arom), 132.40 (1C, s, quart. arom), 131.88 (1C, s, CH arom), 129.44 (1C, s, CH arom), 128.75 (1C, s, CH arom), 127.32 (1C, s, CH arom), 126.66 (1C, s, CH arom), 126.16 (1C, s, CH arom), 125.24 (1C, s, CH arom), 124.11 (1C, s, CH arom), 75.32 (1C, s, $CH_2$ Bn), 72.36 (1C, s, $CH_2$).

**HRMS** calculated for $C_{13}H_{12}O_2$ (200.0837 g/mol): *m/z* 201.0916 $[M+H]^+$; found: *m/z* 201.0910.

**IR** (ATR) $\tilde{\nu}$ = 1736, 1264, 1167, 1097, 980, 792, 775, 731, 702, 422 $cm^{-1}$.

### 5.4.3. Synthesis of Compound **41**

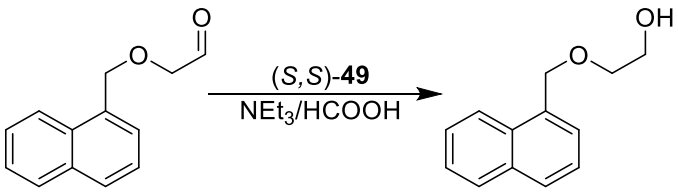


**38** **41**

Compound **41** (0.754 g, 3.7 mmol, 80%) was synthesised according to **general procedure III** using compound **38** (0.943 g, 4.7 mmol, 1 eq.) as starting material. The crude product was purified *via* MPLC [$R_f$ (*n*-heptane:EtOAc = 3:2) = 0.41; gradient 8 % → 90 % EtOAc in *n*-heptane] to give a clear, colourless oil.

**$^1$H NMR** (400.27 MHz, $CDCl_3$ , [42Feb1224/140]): $\delta_H$ 8.13 (1H, d, *J* = 7.67 Hz, CH arom), 7.90-7.80 (2H, m, CH arom), 7.58-7.49 (3H, m, CH arom), 7.45 (1H, q, *J* = 5.0 Hz, CH arom), 5.01 (2H, s, $CH_2$ Bn), 3.76 (2H, t, *J* = 4.71, $CH_2$), 3.69-3.64 (2H, m, $C\underline{H_2}$-OH), 2.12 (1H, broad s, OH).

**$^{13}$C NMR** (100.65 MHz, $CDCl_3$, [42Feb2024/311]): $\delta_C$ 133.92 (1C, s, quart. arom), 133.55 (1C, s, quart. arom), 131.88 (1C, s, CH arom), 129.44 (1C, s, CH arom), 128.75 (1C, s, quart. arom), 127.32 (1C, s, CH arom), 126.66 (1C, s, CH arom), 126.16 (1C, s, CH arom),

125.24 (1C, s, CH arom), 124.11 (1C, s, CH arom), 71.92 (1C, s, $CH_2$ Bn), 71.48 (1C, s, $CH_2$), 62.08 (1C, s, $CH_2$-OH).

### 5.4.4. Synthesis of Compound **44**

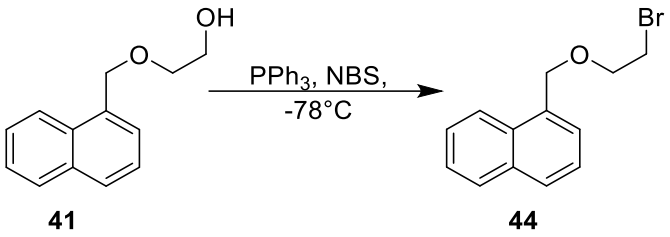


**41** **44**

The synthesis of **44** was performed either according to **general procedure IV – Method A** or **B** using **41** (0.482 g, 2.4 mmol, 1 eq.) as starting material. The crude product was purified *via* MPLC [$R_f$ (*n*-heptane:EtOAc = 1:1) = 0.91; gradient 10 % → 23 % EtOAc in *n*-heptane] to give a copper-brown, clear oil (0.557 g, 2.1 mmol, 89%).

In the case of **Method B,** the product was obtained in quantitative yield albeit with minor impurities.

**$^1$H NMR** (400.27 MHz, $CDCl_3$, [42Feb2724/230]): $\delta_H$ 8.19-8.13 (1H, m, CH arom), 7.90-7.80 (2H, m, 2 × CH arom), 7.58-7.49 (3H, m, 3 × CH arom), 7.45 (1H, q, *J* = 5.0 Hz, CH arom), 5.04 (2H, s, $CH_2$ Bn), 3.86 (2H, t, *J* = 6.2 Hz , $CH_2$), 3.50 (2H, t, *J* = 6.2 Hz, $CH_2$-Br).

**$^{13}$C NMR** (100.65 MHz, $CDCl_3$, [42Feb2724/231]): $\delta_C$ 133.93 (1C, s, quart. arom), 133.27 (1C, s, quart. arom), 131.84 (1C, s, CH arom), 129.93 (1C, s, CH arom), 129.06 (1C, s, CH arom), 128.69 (1C, s, quart. CH arom), 126.80 (1C, s, CH arom), 126.45 (1C, s, CH arom), 126.03 (1C, s, CH arom), 125.30 (1C, s, CH arom), 71.92 (1C, s, $CH_2$ Bn), 70.13 (1C, s, $CH_2$), 31.84 (1C, s, $CH_2$-Br).

**HRMS** calculated for $C_{13}H_{13}OBr$ (264.0150 g/mol): *m/z* 264.0144 $[M\text{-}e^-]^+$; found: *m/z* 264.0136.

**IR** (ATR) $\tilde{\nu}$ = 1274, 1208, 1166, 1033, 791, 772, 734, 574, 515, 407 $cm^{-1}$.

### 5.4.5. Synthesis of Compound **67**

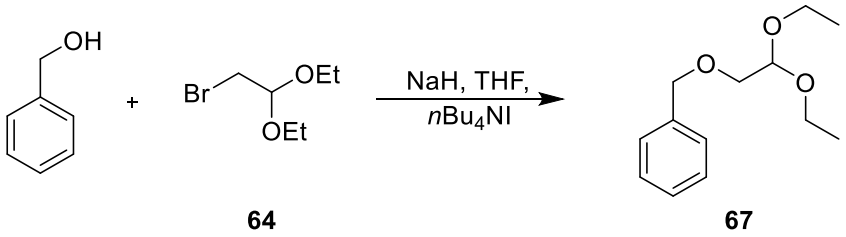


**64** **67**

The synthesis of compound **67** (3.42 g, 15.3 mmol, 76%) was performed using benzyl alcohol (4.16 mL, 40 mmol, 2.0 eq.) according to **general procedure I** to give the product as a clear, orange oil after purification *via* MPLC [$R_f$ (*n*-heptane:EtOAc, 3:2) = 0.52; gradient 10 % → 95 % EtOAc in *n*-heptane].

**$^1$H NMR** ($CDCl_3$ , 400.27 MHz, [42Apr0924/410]): $\delta_H$ 7.39-7.27 (5H, m, CH arom), 4.69 (1H, t, *J* = 5.3 Hz, CH), 4.61 (2H, s, $CH_2$ Bn), 3.63 (4H, 2 × $ABX_3$, A-part: qd, $J_{AB}$ = 9.3 Hz, $J_{AX}$ = 7.1 Hz; B-part : $J_{AB}$ = 9.3 Hz, $J_{BX}$ = 7.1 Hz, 2 × $C\underline{H_2}$-$CH_3$), 3.54 (2H, d, *J* = 5.3 Hz, $CH_2$), 1.25 (6H, t, *J* = 7.1 Hz, 2 × $CH_3$).

### 5.4.6. Synthesis of Compound **62**

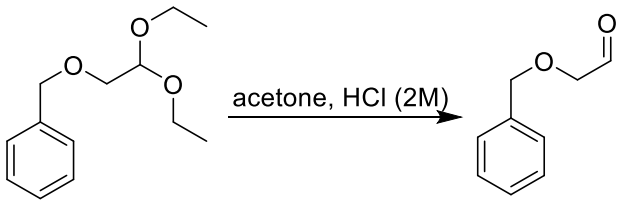


**67** **62**

Compound **67** (3.422 g, 15.3 mmol, 1 eq.) was hydrolysed according to **general procedure II**. The crude residue was purified *via* MPLC [$R_f$ (*n*-heptane:EtOAc = 3:2) = 0.77; gradient 10 % → 80 % EtOAc in *n*-heptane], to give compound **62** (1.034 g, 6.9 mmol, 45%) as a colourless, clear oil.

**$^1$H NMR** (400.27 MHz, $CDCl_3$, [41Apr1624/160]): $\delta_H$ 9.73 (1H, t, *J* = 0.8 Hz, C(O)H), 7.40 – 7.26 (5H, m, CH arom), 4.64 (2H, s, $CH_2$ Bn), 4.11 (2H, d, *J* = 0.8 Hz, $C\underline{H_2}$-C(O)H).

**HRMS** calculated for $C_9H_{10}O_2$ (150.0681 g/mol): *m/z* 149.0603 $[M-H]^-$; found: *m/z* 149.0608.

**IR** (ATR) $\tilde{\nu}$ = 1734, 1454, 1081, 1027, 988, 909, 735, 696, 604, 464 $cm^{-1}$.

### 5.4.7. Synthesis of Compound (*R*)-2-$d_1$-**63** and Compound (*S*)-2-$d_1$-**63**


**62** (*R*)-2-$d_1$-**63**

Compound (*R*)-2-$d_1$-**63** was synthesised according to **general procedure III** starting from **62** (0.632 g, 4.2 mmol, 1 eq.) using deuterated formic acid ($d_1$-**50**, 20 mg, 0.03 mmol, 0.01 eq.) and (*R,R*)-**49** as catalyst. The crude product (0.217 g, 1.4 mmol, 34%) was obtained as clear, colourless oil after purification *via* MPLC [$R_f$ (*n*-heptane:EtOAc, 3:2) = 0.27; gradient 10 % → 95 % EtOAc in *n*-heptane] .

**$^1$H NMR** (400.27 MHz, $CDCl_3$, [42Jun1724/430]): $\delta_H$ 7.38-7.30 (5H, m, CH arom), 4.59 (2H, s, $CH_2$ Bn), 3.77 (1H, broad s, OH), 3.77 – 3.70 (1H, m, $CH_2$-C$\underline{H}$D(OH)), 3.62 (2H, d, *J* = 4.6 Hz, $C\underline{H_2}$-CHD(OH))

**$^{13}$C NMR** (100.65 MHz, $CDCl_3$, [42Jun1724/431]): $\delta_C$ 138.06 (1C, s, $\underline{C}$-$CH_2$ arom), 128.57 (2C, s, CH arom), 127.90 (3C, s, CH arom), 73.39 (1C, s, $CH_2$ Bn), 71.45 (1C, s, $\underline{CH_2}$-CHD(OH)), 61.58 (1C, t, $^1J_{CD}$ = 21.8 Hz, $\underline{C}$HD(OH)).

**HRMS** calculated for $C_9H_{11}DO_2$ (153.0900 g/mol): *m/z* 176.0790 $[M+Na]^+$; found: *m/z* 176.0792.

**IR** (ATR) $\tilde{\nu}$ = 1453, 1275, 1094, 1044, 1027, 938, 736, 715, 698, 610 $cm^{-1}$.

### 5.4.8. Synthesis of Compound **34**

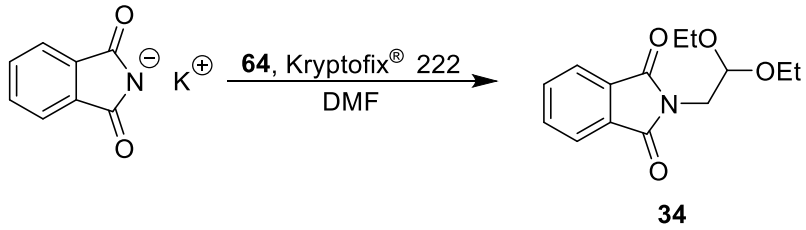


**34**

Potassium phthalimide (3.704 g, 20 mmol, 1.0 eq.) and Kryptofix® 222 (0.30 g, 0.8 mmol 0.057 eq.) were dried *in vacuo* and then dissolved in dry DMF (15 mL). The suspension turned from yellow to orange upon slow addition of bromo acetaldehyde diethyl acetal (**64**, 3.52 mL, 24 mmol, 1.2 eq.). The reaction mixture was stirred at 110°C for 21 hours. The resulting brown suspension was centrifuged (3 × 5 min, 4000 rpm) and the resulting clear solution was washed with DCM (1 × 8 mL). The residue was purified by MPLC [$R_f$ (*n*-heptane:EtOAc = 3:2) = 0.58; gradient 10 % → 59 % EtOAc in *n*-heptane] to give **34** as a colourless crystalline solid (4.676 g, 17.76 mmol, 89 %).

**$^1$H NMR** (400.27 MHz, $CDCl_3$, [41May0824/350]): $\delta_H$ 7.88 – 7.82 (2H, m, 2 × CH arom), 7.75 – 7.69 (2H, m, 2 × CH arom), 4.88 (1H, t, *J* = 5.8 Hz, CH), 3.84 (2H, d, *J* = 5.8 Hz, $CH_2$), 3.62 (4H, $ABX_3$, A-part: qd, $J_{AB}$ = 9.3 Hz, $J_{AX}$ = 7.1 Hz; B-part : $J_{AB}$ = 9.3 Hz, $J_{BX}$ = 7.1 Hz, 2 × $C\underline{H_2}$-$CH_3$), 1.19 (6H, t, *J* = 7.1 Hz, 2 × $CH_2$-$C\underline{H_3}$).

**$^{13}$C NMR** (100.65 MHz, $CDCl_3$, [41May0824/351]): $\delta_C$ 168.24 (2C, s, 2 × N-C(O)), 134.11 (2C, s, 2 × $\underline{C}$-C(O)N), 132.20 (2C, s, 2 × CH arom), 123.46 (2C, s, 2 × CH arom), 98.65 (1C, s, $\underline{C}(OEt)_2$), 61.87 (2C, s, 2 × $\underline{C}H_2$-$CH_3$), 39.94 (1C, s, N-$\underline{C}H_2$), 15.35 (2C, s, 2 × $CH_2$-$\underline{C}H_3$).

**HRMS** calculated for $C_{14}H_{17}NO_4$ (263.1158 g/mol): *m/z* 286.1050 $[M+Na]^+$; found: *m/z* 286.1050.

**IR** (ATR) $\tilde{\nu}$ = 3357, 2486, 2242, 2219, 2272, 1120, 1089, 972, 823, 452 $cm^{-1}$.

### 5.4.9. Synthesis of Compound **37**

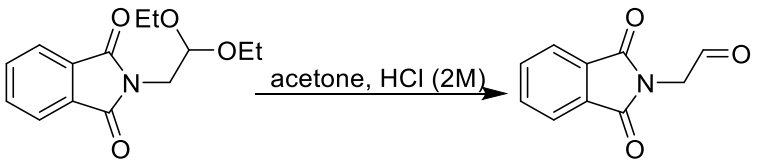


**34** **37**

Diethyl acetal **34** (2.796 g, 10.6 mmol, 1 eq.). was hydrolysed according to **general procedure II.** The product (**37**, 0.955 g, 5.1 mmol, 48%) was obtained as a white crystallin solid after purification *via* MPLC [$R_f$ (*n*-heptane:EtOAc = 3:2) = 0.27; gradient 10 % → 95 % EtOAc in *n*-heptane].

**$^1$H NMR** (400.27 MHz, $CDCl_3$, [41Jul1124/290]): $\delta_H$ 9.66 (1H, s, C(O)H), 7.92 – 7.87 (2H, m, 2 × CH arom), 7.79 – 7.74 (2H, m, 2 × CH arom), 4.56 (2H, s, $CH_2$)

**$^{13}$C NMR** (100.65 MHz, $CDCl_3$, [41Jul1124/291]): $\delta_C$ 193.60 (1C, s, $CH_2$-C(O)H), 167.65 (2C, s, 2 × N-C(O)), 134.49 (2C, s, 2 × C-C(O)N), 132.08 (2C, s, 2 × CH arom), 123.46 (2C, s, 2 × CH arom), 47.51 (1C, s, N-$CH_2$-C(O)H).

**HRMS** calculated for $C_{10}H_6NO_3$ (189.0426 g/mol): *m/z* 188.0350 $[M-H]^-$; found: *m/z* 188.0353.

**IR** (ATR) $\tilde{\nu}$ = 1705, 1405, 1301, 1016, 871, 773, 713, 597, 530, 453$cm^{-1}$

### 5.4.10. Synthesis of Compound **40**

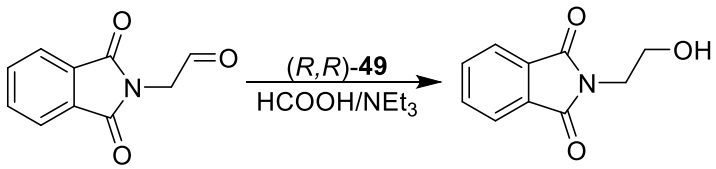


**37** **40**

Compound **40** was synthesised according to **general procedure III** *via* **37** (1.787 g, 2 mmol, 1 eq.). The product was obtained as a colourless solid (0.241 g, 1.3 mmol, 63%) after purification via MPLC [$R_f$ (*n*-heptane:EtOAc = 1:1) = 0.33; gradient 1 % → 80 % EtOAc in *n*-heptane].

**$^1$H NMR** (600.25 MHz, $CDCl_3$, [61Mar1424/100]): $\delta_H$ 7.88 – 7.85 (2H, m, 2 × CH arom), 7.75 – 7.72 (2H, m, 2 × CH arom), 3.93-3.90 and 3.90-3.87 (4H, 2 × m, C$\underline{H_2}$-C$\underline{H_2}$-OH), 2.15 (1H, t, *J* = 5.7 Hz, OH).

**$^{13}$C NMR** ($CDCl_3$, 100.65 MHz, [42Mar1324/232]): $\delta_C$ 168.84 (2C, s, 2 × C(O)), 134.11 (2C, s, 2 × CH arom), 131.96 (2C, s, 2 × quart. C arom), 123.38 (2C, s, 2 × CH arom), 60.92 (1C, s, -$CH_2$-OH), 40.81 (1C, s, N-$CH_2$).

Similarly, (*R*)-*$d_1$*-**40** was synthesized according to **general procedure III** *via* **37** (0.810 g, 4.3 mmol, 1 eq.). The product was obtained as a colourless solid (0.772 g, 4.0 mmol, 94%) after purification via MPLC [$R_f$ (*n*-heptane:EtOAc = 1:4) = 0.50; gradient 10 % → 100 % EtOAc in *n*-heptane].

**$^1$H NMR** (700.40 MHz, $CDCl_3$, [07Apr2424/120]): $\delta_H$ 7.88-7.85 (2H, m, 2 × CH arom), 7.74-7.72 (2H, m, 2 × CH arom), 3.91 (2H, d, *J* = 5.5 Hz, $CH_2$), 3.87 (1H, m, CH), 2.13 (1H, d, OH).

**$^{13}$C NMR** ($CDCl_3$, 100.65 MHz, [07Apr2424/123]): $\delta_C$ 168.84 (2C, s, C(O)), 134.13 (2C, s, CH arom) 131.98 (2C, s, 2 × quart. C arom), 123.42 (2C, s, CH arom), 60.90 (1C, t, $J_{CD}$ = 22.3 Hz C(OH)D), 40.82 (1C, s, N-$\underline{C}H_2$-$CH_2$).

**HRMS** calculated for $C_{10}H_8DNO_3$ (192.0645 g/mol): *m/z* 215.0540 $[M+Na]^+$; found: *m/z* 215.0537.

**IR** (ATR) $\tilde{\nu}$ = 1696, 1468, 1391, 1065, 1011, 985, 722, 533, 437, 404 $cm^{-1}$.

The same reaction was also performed using (*S,S*)-**49** and *d*$_1$-**50** as catalyst to give (*S*)-*d*$_1$-**40** (0.762 g, 4 mmol, 88%). All spectroscopic data were in agreement to those of (*R*)-*d*$_1$-**40** obtained using (*R,R*)-**49** and *d*$_1$-**50**.

### 5.4.11. Synthesis of Compound **43**

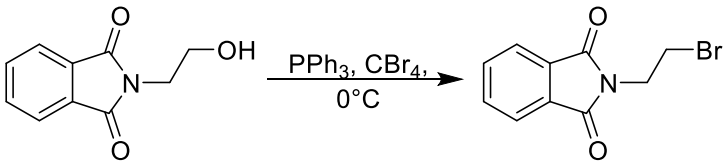


**40** **43**

Compound **43** was synthesised according to **general procedure IV – Method B** from **40** (0.241 g, 1.3 mmol, 1 eq.). The product was obtained as a colourless crystallin solid (0.292 g, 1.2 mmol, 91%) after purification via MPLC [$R_f$ (*n*-heptane:EtOAc = 3:2) = 0.58; gradient 10 % → 90 % EtOAc in *n*-heptane].

**$^1$H NMR** (400.27 MHz, $CDCl_3$, [42Mar2624/320]): $\delta_H$ 7.90-7.85 (2H, m, 2 × CH arom), 7.77-7.70 (2H, m, 2 × CH arom), 4.14 (2H, t, *J* = 6.7 Hz, $C\underline{H_2}$-$CH_2$-Br), 3.65 (2H, t, *J* = 6.7 Hz, $CH_2$-$C\underline{H_2}$-Br).

**HRMS** calculated for $C_{10}H_8BrNO_2$ (252.9738 g/mol): *m/z* 275.9636 $[M+Na]^+$; found: *m/z* 275.9632.

Similarly, (*S*)-*d*$_1$-**43** was synthesized according to **general procedure IV – Method B** *via* (*R*)-*d*$_1$-**40** (0.670 g, 3.5 mmol, 1 eq.). The product was obtained as a colourless crystallin solid (0.840 g, 3.3 mmol, 94%) after purification via MPLC [$R_f$ (*n*-heptane:EtOAc = 1:4) = 0.71; gradient 10 % → 100 % EtOAc in *n*-heptane].

**$^1$H NMR** ($CDCl_3$, 400.27 MHz, [42Apr2324/470]): $\delta_H$ 7.90 (2H, m, 2 × CH arom), 7.77 (2H, m, 2 × CH arom), 4.14 (2H, d, *J* = 6.7 Hz, $CH_2$), 3.63 (1H, t, *J* = 6.7 Hz, CHD-Br).

**$^{13}$C NMR** ($CDCl_3$, 100.65 MHz, [42Apr2324/471]): $\delta_C$ 168.86 (2C, s, C(O)), 134.20 (2C, s, CH arom) 131.99 (2C, s, 2 × quart. C arom), 123.43 (2C, s, 2 × CH arom), 60.90 (1C, t, $J_{CD}$ = 22.6 Hz CBrD), 40.84 (1C, s, N-$\underline{C}H_2$-CHDBr).

**HRMS** calculated for $C_{10}H_7DBrNO_2$ (253.9801 g/mol): *m/z* 253.9796 $[M\text{-}e^-]^+$; found: *m/z* 253.9791.

**IR** (ATR) $\tilde{\nu}$ = 1767, 1705, 1466, 1432, 1391, 1321, 1127, 1039, 982, 802 $cm^{-1}$

### 5.4.12. Synthesis of Compound **46**

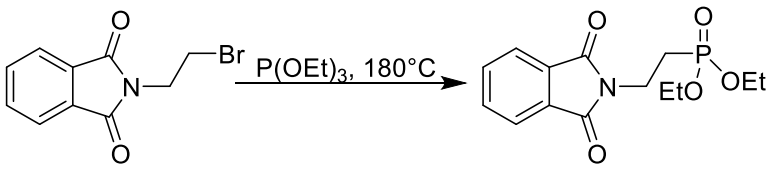


**43** **46**

Phosphonate **46** (0.397 g, 1.3 mmol, 99 mol% purity) was synthesized according to **general procedure V** using **43** (0.292 g, 1.2 mmol, 1 eq.) as starting material. The product was obtained as colourless, clear oil after purification *via* MPLC [Rf (*n*-heptane:EtOAc = 3:2) = 0.50; gradient 10 % → 95 % EtOAc in *n*-heptane].

**$^1$H NMR** (400.27 MHz, $CDCl_3$, [42May0624/190]): $\delta_H$ 7.87-7.81 (2H, m, 2 × CH arom), 7.74 (2H, m, 2 × CH arom), 4.17-4.09 (6H, m, 2 × $CH_2$ OEt + 2H impurity), 4.03-3.94 (2H, ddd, $^3J_{HH}$ = 7.5 Hz, $^2J_{PH}$ = 8.7 Hz, $^3J_{HH}$ = 15.1 Hz, $CH_2$-P), 2.28-2.19 (2H, ddd, $^3J_{PH}$ = 7.5 Hz, $^3J_{HH}$ = 7.5 Hz, 15.1 Hz, $CH_2$-N), 1.36 (3H, t, *J* = 6.9, impurity) 1.32 (6H, t, *J* = 7.7 Hz, 2 × $CH_3$).

**$^{31}$P NMR** (162.03 MHz, $CDCl_3$, [42May0624/191]): $\delta_P$ = 26.74 (s, product, 99 mol%), 33.61 (s, impurity, 1 mol%).

**$^{13}$C NMR** (100.65 MHz, $CDCl_3$, [42Mar1324/192]): $\delta_C$ 167.94 (2C, s, C(O)), 134.16 (2C, s, 2 × CH arom) 132.20 (2C, s, 2 × quart arom), 123.45 (2C, s, CH arom), 62.02 (2C, d, $^3J_{CP}$ = 7.0 Hz, 2 × $\underline{C}H_2$-$CH_3$), 32.34 (1C, d, $^3J_{CP}$ = 2.8 Hz, N-$\underline{C}H_2$-$CH_2$), 24.90 (1C, d, $J_{CP}$ = 140.0 Hz, N-$CH_2$-$\underline{C}H_2$P), 16.48 (2C, d, $^3J_{CP}$ = 6.0 Hz, 2 × $CH_2$-$\underline{C}H_3$).

**HRMS** calculated for $C_{14}H_{18}NO_5P$ (311.0923 g/mol): *m/z* 311.0923 $[M+H]^+$; found: *m/z* 311.0917.

**IR** (ATR) $\tilde{\nu}$ = 1712, 1397, 1362, 1265, 1021, 952, 793, 719, 530, 488 $cm^{-1}$.

### 5.4.13. Synthesis of Mosher esters of Compound (*R*)-*d*$_1$-**40**

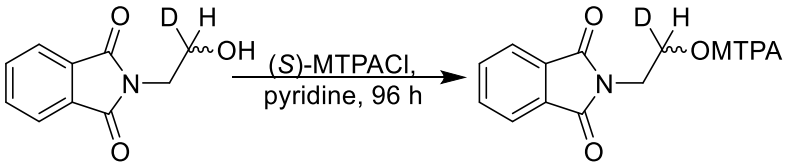


(*R*)-*d*$_1$-**40** (*R*)-Mosher-**40**

The deuterated alcohol (*R*)-*d*$_1$-**40** (19.7 mg, 0.10 mmol), derived from reduction of **37** with (*R,R*)-**49,** was dissolved in dry DCM (2 mL) under argon at room temperature and pyridine (0.25 mL) was added. (*S*)-MTPACl (38.0 mg, 0.15 mmol) was dissolved in DCM (0.5 mL) and added to the reaction mixture. After 96 hours, a 1:1 solution of DCM and 1 M aqueous HCl (20 mL) was added. The phases were separated, the organic layer was washed with a saturated aqueous sodium hydrogen carbonate solution, and dried ($Na_2SO_4$). The residue was purified by MPLC [$R_f$ (*n*-heptane:EtOAc, 1:4) = 0.63; gradient 10 % → 100 % EtOAc in n-heptane] to give (*R*)-Mosher-**40.** [17]

**$^1$H NMR** (700.40 MHz, $CDCl_3$, [7May2324/90]): $\delta_H$ 7.83-7.81 (2H, m, 2 × CH arom Phth), 7.74-7.71 (2H, m, 2 × CH arom Phth), 7.43 (2H, d, *J* = 7.2 Hz, 2 × CH arom MTPA), 7.29-7.25 (3H, m, 3 × CH arom MTPA), 4.56 (1H, q, *J* = 4.7 Hz, CH), 4.04-4.02 (2H, m, $CH_2$), 3.52-3.47 (3H, m, $CH_3O$ MTPA).

Similarly, (*S*)-$d_1$-**40** (19.7 mg, 0.10 mmol) synthesised using (*S,S*)-**49** as a catalyst during the performed asymmetric transfer hydrogenation was converted to (*S*)-Mosher-**40** (yield was equivalent to the other enantioisotopomer).

**$^1$H NMR** (700.40 MHz, $CDCl_3$, [7May2324/80]): $\delta_H$ 7.75 (2H, m, 2 × CH arom Phth), 7.65 (1H, m, 2 ×arom Phth), 7.35 (2H, d, *J* = 7.2 Hz, 2 × CH arom MTPA), 7.22-7.18 (3H, m, 3 × CH arom MTPA), 4.49 (1H, q, *J* = 4.6 Hz, CH), 3.97-3.95 (2H, m $CH_2$), 3.43 (3H, d, *J* = 0.9 Hz, $CH_3O$).

### 5.4.14. Synthesis of Compound **36**

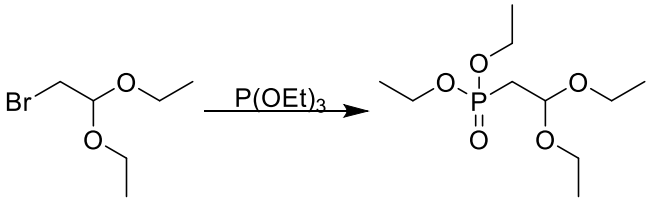


**64** **36**

Compound **36** (5.071 g, 67 mol% purity) was synthesised according to **general procedure V** from **64** (3.941 g, 3.0 mL, 20 mmol). The product was used for the next step without further purification.

**$^1$H NMR** (400.25 MHz, $CDCl_3$, [42May0724/210]): $\delta_H$ 4.84 (1H, q, *J* = 5.6 Hz, CH), 4.04 (4H, q, *J* = 7.2 Hz, 2 × $CH_3C\underline{H_2}OP$),), 3.67-3.56 (2H, m, $CH_3C\underline{H_2}OCH$), 3.55-3.45 (2H, m, $CH_3C\underline{H_2}OCH$), 2.13 (2H, dd, $J_{HH}$ = 18.6 Hz, $J_{HP}$ = 5.6 Hz, 2 × $CH_2$) 1.27 (6H, t, *J* = 7.2 Hz, 2 × $C\underline{H_3}CH_2OP$), 1.15 (6H, t, *J* =7.2 Hz, 2 × $C\underline{H_3}CH_2OCH$).

**$^{31}$P NMR** (162.03 MHz, $CDCl_3$, [42May0724/211]): $\delta_P$ = 26.32 (s).

**HRMS** calculated for $C_{10}H_{23}O_5P$ (254.1283 g/mol): *m/z* 277.1180 $[M+Na]^+$; found: *m/z* 277.1175.

**IR** (ATR) $\tilde{\nu}$ = 2980, 1392, 1249, 1026, 960, 905, 727, 648, 545 $cm^{-1}$.

### 5.4.15. Synthesis of Compound **39**

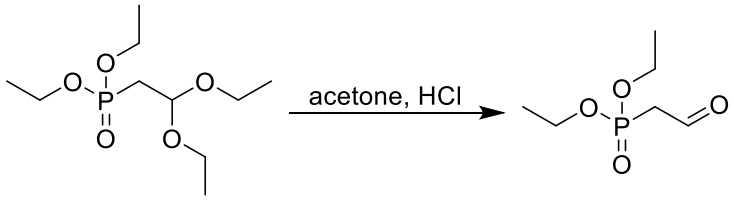


**36** **39**

Compound **39** (2.198 g, 12.2 mmol, 61%) was synthesised according to **general procedure II** from **36** (5.071 g, 20 mmol).

**$^{1}$H NMR** (400.25 MHz, $CDCl_3$, [42May1424/270]): $\delta_H$ 9.69-9.66 (1H, m, C(O)H), 4.14-4.06 (4H, m, 2 × $CH_3C\underline{H_2}OP$), 3.08 (2H, dd, $^{2}J_{PH}$ = 21.8 Hz, $^{3}J_{HH}$ = 3.2 Hz, $PC\underline{H_2}$), 1.19 (3H, t, *J* =7.7, $C\underline{H_3}CH_2OP$), 1.14 (3H, t, *J* = 7.7 Hz, $C\underline{H_3}CH_2OP$)

**$^{31}$P NMR** (162.03 MHz, $CDCl_3$, [42May1424/271]): $\delta_P$ 18.86 (s).

**HRMS** calculated for $C_{14}H_{13}O_4P$ (180.0551 g/mol): *m/z* 203.0440 $[M+Na]^+$; found: *m/z* 203.0444.

### 5.4.16. Synthesis of Compound 2-$d_2$-**42**

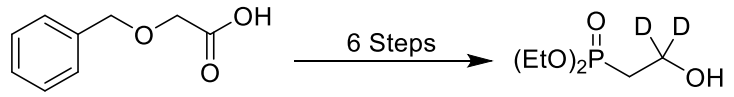


**65** 2-$d_2$-**42**

Compound 2-$d_2$-**42** (0.298 g, 1.6 mmol, 16 % over 6 steps) was synthesised according to the literature from **65** (1.660 g, 1.43 mL, 10 mmol), except that the phosphorous moiety was formed using **general procedure V** with triethyl phosphite at 160°C.[33]

### 5.4.17. Synthesis of Compound **66**

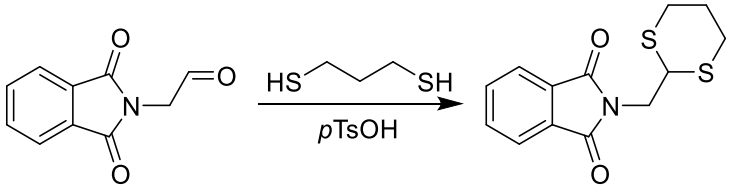


**37** **66**

Compound **37** (1.0 g, 5.3 mmol, 1 eq.) was dissolved in 10 mL dry toluene. *p*TsOH·$H_2O$ (0.1 mg, 0.53 mmol, 0.1 eq.) and 1,3-propanedithiol (0.686 g, 6.3 mmol, 1.2 eq.) were added and the resulting suspension was stirred under reflux for 2.5 h. The reaction mixture was cooled to room temperature and the solvent was removed *in vacuo*. The crude product was redissolved in EtOAc and washed with water, two times with sat. $NaHCO_3$ solution and again with water. Afterwards, the combined aqueous phases were extracted with DCM (two times). The combined organic phases were dried with $Na_2SO_4$ and filtered. The solvent was removed *in vacuo* yielding in compound **66** (1.384 g, 4.95 mmol, 93%) as an off-white solid.

**$^1$H NMR** (600.25 MHz, $CDCl_3$, [42Aug0724/100]): $\delta_H$ 7.89 – 7.84 (2H, m, 2 × CH arom), 7.76 – 7.70 (2H, m, 2 × CH arom), 4.20-4.18 (3H, m, N-C$\underline{H_2}$-C$\underline{H}$), 3.15-3.05 (2H, m, S-C$\underline{H_2}$-$CH_2$), 2.67-2.58 (2H, m, S-C$\underline{H_2}$-$CH_2$), 2.12-2.01 (2H, m, , S-$CH_2$-C$\underline{H_2}$).

### 5.4.18. Synthesis of Compound 2-$d_1$-**39**

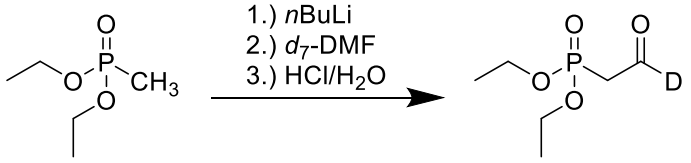


**55** 2-$d_1$-**39**

The synthesis of 2-$d_1$-**39** (1.18 g, 6.4 mmol, 64%) was performed according to literature using $d_7$-DMF (0.881 g, 11.0 mmol, 1.1 eq.) and **55** (1.541 g, 10.0 mmol,1 eq.) as

the starting materials.[29] The reaction mixture was acidified using 3.5 mL HCl (6 M) and extracted 3 times with DCM. The organic phases were combined and dried over $MgSO_4$. Residual starting materials and solvent can be easily removed from the sample by heating at 0.3 mbar.

**$^1$H NMR** (400.27 MHz, $CDCl_3$, [42Sep0524/200]): $\delta_H$ 4.23-4.13 (4H, m, 2 × $CH_3$-C$\underline{H}_2$), 3.07 (2H, d, *J* =21.9 Hz, P-C$\underline{H}_2$-C(O)D), 1.35 (6H, t, *J* =7.0 Hz, 2 × C$\underline{H}_3$-$CH_2$).

**$^{31}$P NMR** (162.03 MHz, $CDCl_3$, [42Sep0524/200]): $\delta_P$ 30.47 (1P, s, educt, 13 mol%), 18.88 (1P, s, product, 87 mol%)

### 5.4.19. Synthesis of Compound 2-$d_1$-**42**

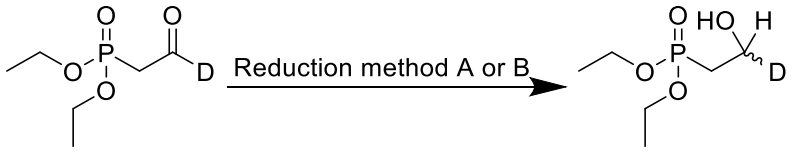


2-$d_1$-**39** 2-$d_1$-**42**

**Reduction Method A – Borane dimethylsulfide and (*R*)-2-Methyloxazaborolidine**

Compound 2-$d_1$-**39** (0.200 g, 1.08 mmol, 1 eq.) and (*R*)-2-methyloxazaborolidine (0.030 g, 0.11 mmol, 0.1 eq.) were suspended in 3 mL abs. THF and cooled to −78°C. Borane dimethylsulfide (0.090 g, 1.19 mmol, 1.1 eq.) in 1 mL THF was added. The reaction mixture was stirred at −78°C for 2.5 h and allowed to warm to −40°C where stirring was continued for 16 h while the reaction mixture was allowed to warm slowly to room temperature. Then, 2 mL methanol were added, and the solvent was removed *in vacuo*. The crude product (2-$d_1$-**42**) was purified using MPLC [$R_f$ (EtOAc) = 0.07; gradient 24 % → 100 % EtOAc in *n*-heptane].

**Reduction Method B – (*R*)-Alpine borane®**

(*R*)-Alpine borane® was freshly prepared from 9-borabicyclo[3.3.1]nonane (0.5 M in THF, 4.32 mL, 2.16 mmol, 2 eq.) and (+)-α-pinene (0.34 mL, 0.294 mg, 2.16 mmol, 2 eq.) under reflux for 3.5 h. The reaction was cooled to room temperature, and the solvent was removed *in vacuo* (40°C at 0.55 mbar). The resulting (*R*)-Alpine borane® was used without further purification.

2-$d_1$-**39** (0.200 g, 1.08 mmol, 1 eq.) was dissolved in 6 mL THF at room temperature under an argon atmosphere. The synthesised (*R*)-Alpine borane® was added in 4 mL THF and stirring was continued for 2 days. Afterwards, acetaldehyde (0.36 mL, 6.5 mmol, 6 eq.) was added and the reaction was stirred for 1.5 h at room temperature. Afterwards, ethanolamine (0.33 mL, 5.4 mmol, 5 eq.) was added and stirred for 2.5 h. The crude reaction mixture was diluted with EtOAc, washed three times with HCl (1M, 20 mL each), three times with saturated aqueous $NaHCO_3$ (20 mL each) and three times with brine (20 mL each). The resulting aqueous phases were combined and concentrated *in vacuo.* The product was obtained by extracting the residue with DCM, drying the organic phase over $MgSO_4$ and removing the remaining solvent *in vacuo*. The crude product was purified via MPLC [$R_f$ (EtOAc) = 0.06; gradient 10 % → 95 % EtOAc in *n*-heptane] to yield 2-$d_1$-**42** (0.086 g, 0.47 mmol, 44%) as colourless oil. [33]

**$^1$H NMR** (400.27 MHz, $CDCl_3$, [42Oct1424/90]): $\delta_H$ 4.19-4.07 (4H, m, 2 × C$\underline{H_2}$-$CH_3$), 3.96-3.81 (1H, m, $CH_2$-C(OH)D$\underline{H}$), 2.80 (1H, broad s, OH), 2.04 (2H, dd, $J_{HH}$ = 6.3 Hz, $J_{HP}$ =17.4 Hz, C$\underline{H_2}$-C(OH)DH), 1.34 (6H, symmetric m, 2 × $CH_2$-C$\underline{H_3}$).

**$^{31}$P NMR** (162.03 MHz, $CDCl_3$, [42Oct1424/91]): $\delta_P$ 30.38 (1P, s).

The enantioisotopomeric excess was determined by the formation of the corresponding Mosher ester from **39** (0.017 g, 0.097 mmol) and (*S*)-MTPA-Cl. (0.5 M in DCM, 2.5 eq.)according to literature. [17] The Mosher ester (0.014 g, 0.035 mmol, 36%) was obtained

after purification *via* MPLC [$R_f$ (*n*-heptane:EtOAc, 1:1) = 0.07; gradient 12 % → 100 % EtOAc in *n*-heptane].

**$^1$H NMR** (400.27 MHz, $C_6D_6$, [42Oct2124/210]): $\delta_H$ 3.92 (∫ 0.058, td, 1H from diastereomer A), 3.78 (∫ 0.942, td, 1H diastereomer B) → ee = 88 %.

## 5.5. Synthesis of the DfmD Substrates

### 5.5.1. Synthesis of Compound **23**

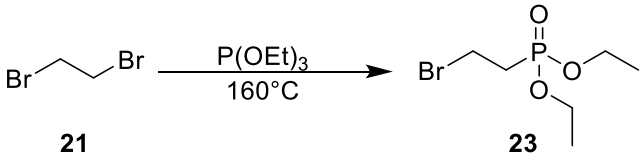


**21** **23**

The Synthesis of **23** was performed according to a literature-known procedure and the product was purified by vacuum distillation (0.6 mbar at 80°C, 2.363 g, 9.6 mmol, 68%). $^{1}$H NMR and $^{13}$C NMR were identical to those reported in the literature.[28]

### 5.5.2. Synthesis of Compound **24**

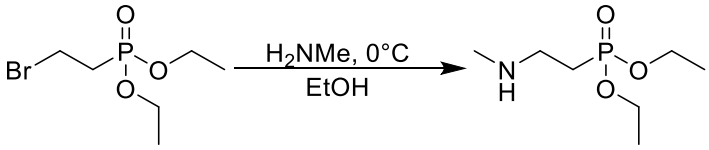


**23** **24**

Compound **24** was synthesised by a literature-known procedure from **23** (0.603 g, 1.5 mmol, 1 eq.) as its hydrobromide salt. The latter was washed with aq. NaOH (20%, 3 × 5 mL). The organic phases were combined, dried ($MgSO_4$) and the solvent removed *in vacuo* to give the product (0.315 g, 1.5 mmol, quant.) as a clear, colourless oil. $^{1}$H NMR and $^{13}$C NMR were equal to the literature.[28]

### 5.5.3. Synthesis of Compound **25**

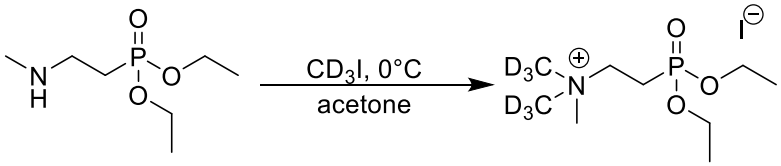


**24** **25**

$CD_3I$ (1.68 mL, 20 mmol, 4 eq.) was slowly added to compound **24** (0.976 g, 5 mmol, 1 eq.) dissolved in dry acetone (8 mL) under an argon atmosphere at 0°C. The reaction was allowed to warm to room temperature while stirring. After a few seconds, the formation of a white solid was observed. The reaction was stirred for 16 h at room temperature. The solid was filtered over cotton, washed 3 times with acetone and redissolved in water. The solvent was removed *in vacuo* to obtain **25** as its iodide salt (0.216 g, 0.6 mmol, 12%) as an off-white solid.

**$^1$H NMR** (600.25 MHz, $D_2O$, [61Aug0824/40]): $\delta_H$ 4.26-4.19 (4H, m, 2 × $C\underline{H_2}$-$CH_3$), 3.65-3.60 (2H, m, N-$C\underline{H_2}$-$CH_2$-P), 3.17 (3H, s, N-$CH_3$), 2.54 (2H, symmetric m, N-$CH_2$-$C\underline{H_2}$-P), 1.37 (6H, t, $^3J_{HH}$ = 7.1 Hz, 2 × $CH_2$-$C\underline{H_3}$).

**$^{31}$P NMR** (242.99 MHz, $D_2O$, [61Aug0824/41]): $\delta_P$ 27.25 (1P, t, $^3J_{PN}$ = 7.0 Hz).

**$^{13}$C NMR** (150.93 MHz, $D_2O$, [61Aug0824/42]): $\delta_C$ 64.14 (2C, d, $^2J_{CP}$=6.5 Hz, 2 × $\underline{C}H_2$-$CH_3$), 60.03 (1C, s, N-$\underline{C}H_2$-$CH_2$-P), 52.57 (1C, broad s, N-$CH_3$), 52.99-51.60 (2C, m, 2 × $CD_3$), 19.64 (1C, d, $^1J_{CP}$ = 138.4 Hz, N-$CH_2$-$\underline{C}H_2$-P), 15.53 (2C, d, $^3J_{CP}$ = 6.5 Hz, 2 × $CH_2$-$\underline{C}H_3$).

**HRMS** calculated for $C_9H_{17}D_6INO_3P$ (357.0837 g/mol): *m/z* 230.1792 $[M\text{-}I]^+$; found: *m/z* 230.17867.

**IR** (ATR) $\tilde{\nu}$ = 3438, 2980, 2759, 1459, 1391, 1217, 1160, 1098, 1014, 963 $cm^{-1}$

### 5.5.4. Synthesis of Compound *d*$_6$-**17**

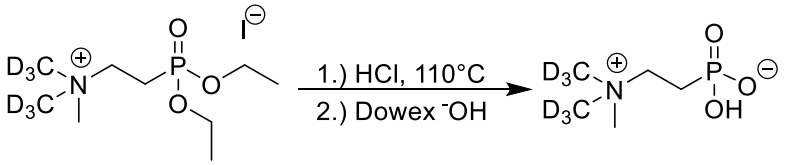


**25** *d*$_6$-**17**

Deprotection of **25** (0.216 g, 0.6 mmol, 1 eq.) was performed according to literature to obtain *d*$_6$-**17** (0.028 g, 0.2 mmol, 27%) as colourless crystals.[28]

**$^1$H NMR** (600.25 MHz, $D_2O$, [42Sep1924/60]): $\delta_H$ 3.70-3.62 (2H, m, N-C$\underline{H_2}$-$CH_2$-P), 3.21 (3H, s, N-$CH_3$), 2.57 (2H, symmetric m, N-$CH_2$-C$\underline{H_2}$-P).

**$^{31}$P NMR** (242.99 MHz, $D_2O$, [42Sep1924/61]): $\delta_P$ 17.11 (1P, t, $^3J_{PN}$ = 7.2 Hz).

**$^{13}$C NMR** (150.93 MHz, $D_2O$, [42Sep1924/62]): 59.71 (1C, s, N-$\underline{C}H_2$-$CH_2$-P), 53.36 (1C, broad s, N-$CH_3$), 52.37-52.20 (2C, m, 2 × $CD_3$), 23.27 (1C, d, $^1J_{CP}$ = 138.4 Hz, N-$CH_2$-$\underline{C}H_2$-P).

**HRMS** calculated for $C_5H_8D_6NO_3P$ (173.1088 g/mol): *m/z* 196.0986 $[M+Na]^+$; found: *m/z* 196.09801.

**IR** (ATR) $\tilde{\nu}$ = 2980, 2593, 1441, 1393, 1236, 1160, 1140, 1100, 1016, 959 $cm^{-1}$

### 5.5.5. Synthesis of Compound **26**

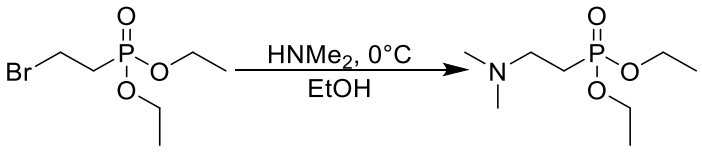


**23** **26**

The synthesis of compound **26** (1.429 g, 5.8 mmol, 1 eq.) was performed according to the literature. The crude product was washed 3 times with 5 mL of NaOH (20%). The organic phase was dried over $Na_2SO_4$, filtered *via* cotton and the solvent was removed *in vacuo*. Compound **26** (1.182 g, 5.5 mmol, 97%) was obtained as a clear, colourless oil.$^{1}$H NMR and $^{13}$C NMR were identical to the literature.[28]

### 5.5.6. Synthesis of Compound **27**

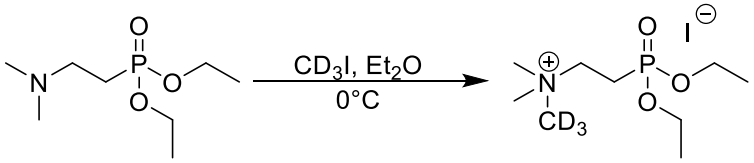


**26** **27**

Compound **26** (0.348 g, 1.7 mmol, 1 eq.) was reacted with $CD_3I$ according to the literature. Compound **27** (0.437 g, 1.2 mmol, 74%) was obtained as a clear colourless solid.

**$^{1}$H NMR** (600.25 MHz, $D_2O$, [61Aug0924/60]): $\delta_H$ 4.26-4.19 (4H, m, 2 × C$\underline{H_2}$-$CH_3$), 3.65-3.60 (2H, m, N-C$\underline{H_2}$-$CH_2$-P), 3.17 (6H, s, 2 × N-$CH_3$), 2.54 (2H, symmetric m, N-$CH_2$-C$\underline{H_2}$-P), 1.37 (6H, t, $^{3}J_{HH}$= 7.1 Hz, 2 × $CH_2$-C$\underline{H_3}$).

**$^{31}$P NMR** (242.99 MHz, $D_2O$, [61Aug0924/67]): $\delta_P$ 27.25 (1P, t, $^{3}J_{PN}$ = 5.9 Hz).

**$^{13}$C NMR** (150.93 MHz, $D_2O$, [61Aug0924/66]): $\delta_C$ 64.14 (2C, d, $^{2}J_{CP}$=7.9 Hz, 2 × $\underline{C}H_2$-$CH_3$), 60.14 (1C, s, N-$\underline{C}H_2$-$CH_2$-P), 52.58 (2C, broad s, 2 × N-$CH_3$), 52.09-51.71 (1C, m, $CD_3$), 19.69 (1C, d, $^{1}J_{CP}$=138.4 Hz, N-$CH_2$-$\underline{C}H_2$-P), 15.54 (2C, d, $^{3}J_{CP}$ = 6.5 Hz, 2 × $CH_2$-$\underline{C}H_3$).

**HRMS** calculated for $C_9H_{20}D_3INO_3P$ (354.0649 g/mol): *m/z* 227.1604 $[M\text{-}I]^+$; found: *m/z* 227.15984.

**IR** (ATR) $\tilde{\nu}$ = 2963, 1495, 1238, 1015, 967, 845, 795, 791, 761 $cm^{-1}$

### 5.5.7. Synthesis of Compound *d*$_3$-**17**

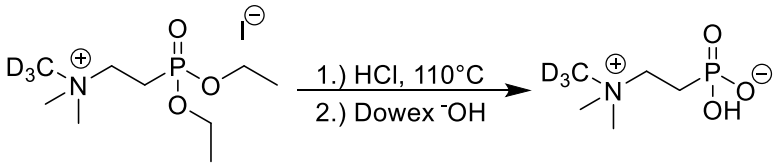


**27** *d*$_3$-**17**

Compound **27** (0.437 g, 1.2 mmol, 1 eq.) was deprotected according to the literature to give *d*$_3$-**17** (0.197 g, 1.15 mmol, 94%) as colourless crystals.[28]

**$^1$H NMR** (400.27 MHz, $D_2O$, [42Jul2924/190]): $\delta_H$ 3.65-3.60 (2H, m, N-C$\underline{H_2}$-$CH_2$-P), 3.17 (6H, s, N-$CH_3$), 2.54 (2H, symmetric m, N-$CH_2$-C$\underline{H_2}$-P).

**$^{31}$P NMR** (162.03 MHz, $D_2O$, [42Jul2924/191]): $\delta_P$ 27.25 (1P, t, $^3J_{PN}$ = 5.9 Hz).

**IR** (ATR) $\tilde{\nu}$ = 2994, 2652, 1458, 1393, 1236, 1172, 1120, 1100, 1012, 752 cm$^{-1}$

## 5.6. Stopped-flow Measurements and enzymatic Assays

Analysis of the FfnD and DfmD substrates followed literature procedures.[36,37] The protein sequence and the used buffer can be found in Appendix A.

### 5.6.1. FfnD QQQ-MS Assay of the Compounds (S)-$d_1$-**19** and **19**

0.4 mM Fe(II) chloride, 0.44 mM enzyme, 2 mM substrate, and varying concentrations 2-oxoglutaric acid (2OG) were mixed 1:1 with air saturated buffer (4°C, 0.38 mM $O_2$) to a total volume of 1 mL

Sample1: 0 mM 2OG

Sample 2: 1 mM 2OG

Sample 3: 2 mM 2OG

Sample 4: 4 mM 2OG

Sample 5: 10 mM 2OG.

The samples were allowed to stir overnight at 4°C, then mixed again 1:1 against acetonitrile to quench the reaction. The final (observed) concentrations are 1/4 of initial concentrations. The reaction mixtures were centrifuged for 5 min at 14000 × g. The supernatants were placed in 10 kDa spin filter and spun again 5 min at 14000 × g. The flow-through was collected as sample. After the SIM/Scan method was finished, 10:1 NaSCN:2OG was added to reduce any remaining 2OG to 2-hydroxyglutarate (100 mM stock of NaSCN, added to 100 µL of sample). The samples were run again on MRM method to quantify the succinate production.

### 5.6.2. FfnD NMR Assay of the Compounds (S)-*d*$_1$-**19** and **19**

Reaction mixtures with the concentration of 0.4 mM Fe(II)chloride, 0.44 mM enzyme, 6 mM substrate [(S)-*d*$_1$-**19** or **19**] and varying 2OG amounts were mixed 1:1 against air saturated buffer (4°C, 0.38 mM $O_2$).

Sample 1: 0 mM 2OG

Sample 2: 20 mM 2OG.

The final (observed) concentrations equal half of the initial concentrations. The samples were spiked with 50 µL of $D_2O$ for signal locking. The reaction mixture was allowed to sit for 4 h at room temperature before spectra were recorded.

### 5.6.3. FfnD Stopped flow Measurements of the Compounds (S)-*d*$_1$-**19** and **19**

A sample containing the following concentrations was prepared: 1 mM Fe(II)chloride, 1.1 mM enzyme, 4 mM substrate [(S)-*d*$_1$-**19** or **19**], 8 mM 2OG mixed 1:1 against air saturated buffer (4°C, 0.38 mM $O_2$). Final (observed) concentrations are half of the initial concentrations.

### 5.6.4. DfmD QQQ-MS Assay of the Compounds *d*$_3$-**17** and **17**

Reaction mixtures with the concentration of 1mM Fe(II)chloride, 1.1 mM enzyme, 1 mM substrate (*d*$_3$-**17** or **17**), varying 2OG mixed 1:1 against air saturated buffer (4℃, 0.38 mM $O_2$) were prepared.

Sample1: 0 mM 2OG

Sample 2: 0.5 mM 2OG

Sample 3: 1 mM 2OG

Sample 4: 2 mM 2OG

Sample 5: 5 mM 2OG.

The samples were allowed to stir overnight at 4°C, then mixed again 1:1 against acetonitrile to quench the reaction. The final (observed) concentrations are 1/4 of initial concentrations. The reaction mixtures were centrifuged for 5 min at 14000 × g. The supernatants were placed in 10 kDa spin filter and spun again 5 min 14000 × g. The flow-through was collected as sample. After the SIM/Scan method was finished, 10:1 NaSCN:2OG was added to reduce any remaining 2OG to 2-hydroxyglutarate (100 mM stock of NaSCN, added to 100 µL of sample). The samples were run again on MRM method to quantify the succinate production.

### 5.6.5. DfmD NMR Assay of the Compounds *d*$_3$-**17** and **17**

Reaction mixtures with the concentration of 0.4 mM Fe(II) chloride, 0.53 mM enzyme, 6 mM substrate (*d*$_3$-**17** or **17**), varying 2OG mixed 1:1 against air saturated buffer (4℃, 0.38 mM $O_2$) were prepared.

Sample 1: 0 mM 2OG

Sample 2: 20 mM 2OG.

The final (observed) concentrations equal half of the initial concentrations. The samples were spiked with 50 µL of $D_2O$ for signal locking. The reaction mixture was allowed to sit for 4 h at room temperature before NMR spectra were recorded.

### 5.6.6. DfmD Stopped flow Measurements of the Compounds *d*$_3$-**17** and **17**

A sample containing the following concentrations was prepared: 1 mM Fe(II) chloride, 1.1 mM enzyme, 4 mM substrate (*d*$_3$-**17** or **17**), 8 mM 2OG mixed 1:1 against air saturated buffer (4°C, 0.38 mM $O_2$) and also oxygen saturated buffer (4°C, 1.8 mM $O_2$). The final (observed) concentrations are half of initial.

# 6. Abstract

This thesis focuses on the synthesis of deuterated substrate analogues for the enzymes DfmD, FfnD, and TmpA, and on mechanistic studies on these non-heme iron(II) and 2-oxoglutarate-dependent oxygenases using the synthesised substrates. All of these enzymes catalyse unusual transformations in phosphonate biosynthetic pathways. The study aims at clarifying their mechanisms, particularly their unique ability to diverge from typical oxygen rebound reactions, and to catalyse transformations such as epoxidations, desaturations, and demethylations instead. This work addresses the challenges of achieving high enantioisotopic purity, while minimising costs through efficient incorporation of deuterium labels using atom-economic, synthetic pathways.

To achieve these aims, multiple synthetic strategies either using all-*protio* substrates in combination with asymmetric transfer deuteration or deuterated aldehydes in combination with stereoselective, catalytic reductions using varied borane reagents were tried. Additionally, various analytical methods were employed to determine the enantioisotopomeric excess of the obtained compounds, including the use of chiral solvating agents and derivatization strategies in combination with nuclear magnetic resonance (NMR) spectroscopy.

Enzyme assays utilizing the synthesised deuterated compounds were conducted to explore kinetic isotope effects (KIE) and to observe isotope-sensitive steps in the enzyme catalytic cycles. Stopped-flow-methods (with UV/Vis-spectroscopy detection), mass spectrometry (MS), and nuclear magnetic resonance (NMR) assays were key techniques in measuring these effects, revealing significant details of the coupling efficiency of the target enzymes and of the intermediate formation. Results, which only became possible using the target compounds, indicate that deuterium incorporation affects bond dissociation at critical points, slowing reaction rates and potentially impacting enzyme-substrate coupling efficiency.

Thus, this study both provides new insights on potential strategies for deuterium incorporation in a site- and stereoselective way and contributes to a deeper understanding of phosphonate biosynthetic enzymes.

# 7. Deutsche Zusammenfassung

Die vorliegende Arbeit konzentriert sich auf die Synthese und die mechanistische Untersuchung Deuterium-markierter Substrate der Enzyme DfmD, FfnD und TmpA (non-heme iron(II) and 2-oxoglutarate-dependent Oxygenasen), die außergewöhnliche Transformationen in Phosphonat-Biosynthesewegen katalysieren. Die vorliegende Arbeit soll zur Erforschung der Mechanismen dieser Enzyme beitragen. Insbesondere deren Fähigkeit, einen typischen "Oxygen-Rebound" zu unterdrücken und stattdessen Epoxidierungen, Desaturierungen und Demethylierungen zu katalysieren, soll näher untersucht werden. Die Synthese der isotopenmarkierten Zielsubstanzen war vor allem unter Berücksichtigung (atom-)ökonomischer Aspekte von Interesse für diese Arbeit.

Enzymassays unter Verwendung der synthetisierten Deuterium-markierten Substrate wurden durchgeführt, um die resultierenden kinetischen Isotopeneffekte (KIE) zu untersuchen. Stopped-Flow-Methoden, Massenspektrometrie (MS) und NMR-Analysen waren zentrale Techniken zur Messung dieser Effekte und ermöglichten Einblicke in die Enzymeffizienz. Die Ergebnisse legen nahe, dass der Isotopenaustausch spezifische Bindungsbrüche, die an kritischen Reaktionsschritte beteiligt sind, sowie die Enzym-Substrat Bindung beeinflussen.

Die vorliegende Arbeit trägt daher sowohl zu einem besseren Verständnis der Phosphonatbiosynthese, als auch zur Entwicklung neuer Strategien zur Deuterium-Markierung bei.

# 8. References


(1) Elsevier. *Scopus*. https://www-scopus-com/ (accessed 2024-09-23).

(2) Schipanski, M. E.; Bennett, E. M. The Phosphorus Cycle. In *Fundamentals of Ecosystem Science*; Elsevier, **2021**; pp 189–213. DOI: 10.1016/B978-0-12-812762-9.00009-5.

(3) Menge, D. N.; Kou-Giesbrecht, S.; Taylor, B. N.; Akana, P. R.; Butler, A.; Carreras Pereira, K. A.; Cooley, S. S.; Lau, V. M.; Lauterbach, E. L. Terrestrial Phosphorus Cycling: Responses to Climatic Change. *Annu. Rev. Ecol. Evol. Syst.* **2023**, *54* (1), 429–449. DOI: 10.1146/annurev-ecolsys-110421-102458.

(4) Correll, D. L. The Role of Phosphorus in the Eutrophication of Receiving Waters: A Review. *J of Env Quality* **1998**, *27* (2), 261–266. DOI: 10.2134/jeq1998.00472425002700020004x.

(5) Smil, V. PHOSPHORUS IN THE ENVIRONMENT: Natural Flows and Human Interferences. *ANNU REV ENERG ENV* **2000**, *25*, 53–88. DOI: 10.1146/annurev.energy.25.1.53.

(6) Walsh, C. T. *The chemical biology of phosphorus*; Chemical biology, Vol. 13; Royal Society of Chemistry, **2021**. DOI: 10.1039/9781839162312.

(7) Westheimer, F. H. Why Nature Chose Phosphates. *Science* **1987** (235), 1173–1178. DOI: 10.1126/science.2434996.

(8) Barenholz, Y.; Thompson, T. E. Sphingomyelin: biophysical aspects. *Chemistry and physics of lipids* **1999**, *102* (1-2), 29–34. DOI: 10.1016/S0009-3084(99)00072-9.

(9) *Biochemistry of Lipids, Lipoproteins and Membranes*:*Chapter 7 - Phospholipid Synthesis in Mammalian Cells*; Elsevier, **2016**. DOI: 10.1016/B978-0-444-63438-2.00007-9.

(10) Metcalf, W. W.; van der Donk, W. A. Biosynthesis of phosphonic and phosphinic acid natural products. *Annual review of biochemistry* **2009**, *78*, 65–94. DOI: 10.1146/annurev.biochem.78.091707.100215.

(11) Furtak, A.; Szafranek-Nakonieczna, A.; Furtak, K.; Pytlak, A. A review of organophosphonates, their natural and anthropogenic sources, environmental fate and impact on microbial greenhouse gases emissions - Identifying knowledge gaps. *Journal of environmental management* **2024**, *355*, 120453. DOI: 10.1016/j.jenvman.2024.120453. Published Online: Mar. 1, 2024.

(12) Boden, J. S.; Zhong, J.; Anderson, R. E.; Stüeken, E. E. Timing the evolution of phosphorus-cycling enzymes through geological time using phylogenomics. *Nature communications* **2024**, *15* (1), 3703. DOI: 10.1038/s41467-024-47914-0. Published Online: May. 2, 2024.

(13) Liang, Z.; McCabe, K.; Fawcett, S. E.; Forrer, H. J.; Hashihama, F.; Jeandel, C.; Marconi, D.; Planquette, H.; Saito, M. A.; Sohm, J. A.; Thomas, R. K.; Letscher, R. T.; Knapp, A. N. A global ocean dissolved organic phosphorus concentration database (DOPv2021). *Scientific data* **2022**, *9* (1), 772. DOI: 10.1038/s41597-022-01873-7. Published Online: Dec. 16, 2022.

(14) Li, S.; Horsman, G. P. An inventory of early branch points in microbial phosphonate biosynthesis. *Microbial genomics* **2022**, *8* (2). DOI: 10.1099/mgen.0.000781.

(15) Pallitsch, K.; Zechel, D. L. The functional importance of bacterial oxidative phosphonate pathways. *Biochemical Society transactions* **2023**, *51* (2), 487–499. DOI: 10.1042/BST20220479.

(16) Hammerschmidt, F. Biosynthese von Naturstoffen mit einer P□C-Bindung. III. Synthese der (R )- und (S )-(2-Amino[1-D 1 ]ethyl)phosphonsäure und deren Hydroxylierung zu (2-Amino-1-hydroxyethyl)phosphonsäure in Acanthamoeba castellanii (Neff). *Liebigs Ann. Chem.* **1988**, *1988* (10), 955–960. DOI: 10.1002/jlac.198819881004.

(17) Hammerschmidt, F.; Kaehlig, H. Biosynthesis of natural products with a phosphorus-carbon bond. 7. Synthesis of [1,1-2H2]-, [2,2-2H2]-, (R)- and (S)-[1-2H1](2-hydroxyethyl)phosphonic acid and (R,S)-[1-2H1](1,2-dihydroxyethyl)phosphonic acid and incorporation studies into fosfomycin in Streptomyces fradiae. *J. Org. Chem.* **1991**, *56* (7), 2364–2370. DOI: 10.1021/jo00007a022.

(18) Dinhof, T. On the synthesis of potentially bioactive, chiral aminophosphonic acids. master thesis, University of Vienna, Vienna, **2021**.

(19) Rowbotham, J. S.; Ramirez, M. A.; Lenz, O.; Reeve, H. A.; Vincent, K. A. Bringing biocatalytic deuteration into the toolbox of asymmetric isotopic labelling techniques. *Nature communications* **2020**, *11* (1), 1454. DOI: 10.1038/s41467-020-15310-z. Published Online: Mar. 19, 2020.

(20) Kopf, S.; Bourriquen, F.; Li, W.; Neumann, H.; Junge, K.; Beller, M. Recent Developments for the Deuterium and Tritium Labeling of Organic Molecules. *Chemical reviews* **2022**, *122* (6), 6634–6718. DOI: 10.1021/acs.chemrev.1c00795. Published Online: Feb. 18, 2022.

(21) Vang, Z. P.; Hintzsche, S. J.; Clark, J. R. Catalytic Transfer Deuteration and Hydrodeuteration: Emerging Techniques to Selectively Transform Alkenes and Alkynes to Deuterated Alkanes. *Chemistry (Weinheim an der Bergstrasse, Germany)* **2021**, *27* (39), 9988–10000. DOI: 10.1002/chem.202100635. Published Online: Jun. 9, 2021.

(22) Beck, A. K.; Dahinden, R.; Kühnle, F. N. M. Tartrate-Derived Ligands for the Enantioselective LiAlH 4 Reduction of Ketones. In *Reductions in Organic Synthesis*;

Abdel-Magid, A. F., Ed.; ACS Symposium Series; American Chemical Society, **1996**; pp 52–69. DOI: 10.1021/bk-1996-0641.ch003.

(23) Ramalingam, K.; Nanjappan, P.; Kalvin, D. M.; Woodard, R. W. A practical large scale chemical synthesis of chiral glycines. *Tetrahedron* **1988**, *44* (17), 5597–5604. DOI: 10.1016/S0040-4020(01)86064-6.

(24) Mills, M. D.; Sonstrom, R. E.; Vang, Z. P.; Neill, J. L.; Scolati, H. N.; West, C. T.; Pate, B. H.; Clark, J. R. Enantioselective Synthesis of Enantioisotopomers with Quantitative Chiral Analysis by Chiral Tag Rotational Spectroscopy. *Angewandte Chemie (International ed. in English)* **2022**, *61* (33), e202207275. DOI: 10.1002/anie.202207275. Published Online: Jul. 8, 2022.

(25) Yang, L.; Wenzel, T.; Williamson, R. T.; Christensen, M.; Schafer, W.; Welch, C. J. Expedited Selection of NMR Chiral Solvating Agents for Determination of Enantiopurity. *ACS central science* **2016**, *2* (5), 332–340. DOI: 10.1021/acscentsci.6b00062. Published Online: Apr. 20, 2016.

(26) Sonstrom, R. E.; Vang, Z. P.; Scolati, H. N.; Neill, J. L.; Pate, B. H.; Clark, J. R. Rapid Enantiomeric Excess Measurements of Enantioisotopomers by Molecular Rotational Resonance Spectroscopy. *Organic process research & development* **2023**, *27* (7), 1185–1197. DOI: 10.1021/acs.oprd.3c00028. Published Online: Mar. 17, 2023.

(27) Almeida, P. *Proteins*:*Concepts in Biochemistry*; Taylor & Francis Group, **2016**.

(28) Zangelmi, E.; Ruffolo, F.; Dinhof, T.; Gerdol, M.; Malatesta, M.; Chin, J. P.; Rivetti, C.; Secchi, A.; Pallitsch, K.; Peracchi, A. Deciphering the role of recurrent FAD-dependent enzymes in bacterial phosphonate catabolism. *iScience* **2023**, *26* (11), 108108. DOI: 10.1016/j.isci.2023.108108. Published Online: Oct. 4, 2023.

(29) Aboujaoude, E. E.; Collignon, N.; Savignac, P. A Simple Synthesis of Dialkyl 1-Formylalkanephosphonates. *Synthesis* **1983**, *1983* (08), 634–636. DOI: 10.1055/S-1983-30452.

(30) Kuethe, J. T. Synthesis of stable isotope-labeled metabolites of asenapine. *Labelled Comp Radiopharmac* **2012**, *55* (5), 180–185. DOI: 10.1002/jlcr.2924.

(31) Li, W.; Li, J.; Lin, M.; Wacharasindhu, S.; Tabei, K.; Mansour, T. S. Dimethyl sulfoxide mediated elimination reactions in 3-aryl 2,3-dihalopropanoates: scope and mechanistic insights. *J. Org. Chem.* **2007**, *72* (16), 6016–6021. DOI: 10.1021/jo070217c. Published Online: Jul. 12, 2007.

(32) Peng, J.; Jiang, X.; Guo, X.; Zhao, D.; Ma, Y. Sensitizer design for efficient triplet-triplet annihilation upconversion: annihilator-appended tris-cyclometalated Ir(III) complexes. *Chemical communications (Cambridge, England)* **2014**, *50* (58), 7828–7830. DOI: 10.1039/c4cc01465k.

(33) Wang, B.; Blaszczyk, A. J.; Knox, H. L.; Zhou, S.; Blaesi, E. J.; Krebs, C.; Wang, R. X.; Booker, S. J. Stereochemical and Mechanistic Investigation of the Reaction Catalyzed by Fom3 from Streptomyces fradiae, a Cobalamin-Dependent Radical S-Adenosylmethionine Methylase. *Biochemistry* **2018**, *57* (33), 4972–4984. DOI: 10.1021/acs.biochem.8b00693. Published Online: Aug. 9, 2018.

(34) van Staalduinen, L. M.; McSorley, F. R.; Schiessl, K.; Séguin, J.; Wyatt, P. B.; Hammerschmidt, F.; Zechel, D. L.; Jia, Z. Crystal structure of PhnZ in complex with substrate reveals a di-iron oxygenase mechanism for catabolism of organophosphonates. *Proceedings of the National Academy of Sciences of the United States of America* **2014**, *111* (14), 5171–5176. DOI: 10.1073/pnas.1320039111. Published Online: Mar. 21, 2014.

(35) Stankovic, T. Synthesis of potentially bioactive compounds, University of Vienna, Vienna, **2019**.

(36) Li, X.; Xue, S.; Guo, Y.; Chang, W.-C. Mechanism of Methyldehydrofosmidomycin Maturation: Use Olefination to Enable Chain Elongation. *Journal of the American Chemical Society* **2022**, *144* (18), 8257–8266. DOI: 10.1021/jacs.2c01924. Published Online: Apr. 28, 2022.

(37) Gama, S. R.; Stankovic, T.; Hupp, K.; Al Hejami, A.; McClean, M.; Evans, A.; Beauchemin, D.; Hammerschmidt, F.; Pallitsch, K.; Zechel, D. L. Biosynthesis of the Fungal Organophosphonate Fosfonochlorin Involves an Iron(II) and 2-(Oxo)glutarate Dependent Oxacyclase. *Chembiochem : a European journal of chemical biology* **2022**, *23* (2), e202100352. DOI: 10.1002/cbic.202100352. Published Online: Sep. 20, 2021.

# 9. List of Figures

# 10. Appendix – Protein Sequences

**FfnD Sequence**

ATGGCGCCGGGTCTGATCGAAACCGTTTCTGATTTCTCTCACCTGCCGAAAACCGA
TACCGTACCAAACTGGAAGTTAAACCGAAATCTGCTCTGTTCCCGGATGGTTACAAA
ACCACCGGCCAGCAGCCGCCGCTGTATGAAGAAATCCACCCGTACTCCGACTTCCC
GAAGAAAATCACCGGCATCACCGCGTGGACCAAAGATGACCTGAGCGGTTCTCCG
GAAAAAGAAGCAATCTGGAAACACCCGTTCACCGAAGAAGAACTGGAAGATCTGTC
TACCGCGGCGGAAAACTACATCAACTCTGGTCGTGACCTGAACGAAATGTGCAAAG
AACTGTTCCCGCTGCCGCGTATGGAAAAATACCTGGAAGAAGTTCGTGACGACATG
ATCAACGGCTACGGTTTCATCCTGTTCCAGGGTATGCCGGTTAAAGAATGGGGTATG
CGTAAATCTTCCACCGCGTACATGGGTCTGGGCGCGCACTTCGGTCACATCGTGTC
CCAGAACGGTCGTGGTCACGTTCTGGGCCACATCAAAGACCTGGGTGAAAACCCG
GCGGATTTCCACAAAGTTCGTCTGTACCGTACCACCGCGCGTCAGACCTTCCACGC
GGACCCGGCTGACATCGTGGGTCTGCTGTGCCTGAACACCCCGCTGAAAGGTGGT
GAAAACAACATCGTTTCCGGTCACCGTGTTTGGAACGTGATGCAGGAAGAACGCCC
GGACATCGCAGAACTGCTGACCCAGCCGATCTGGTACTTCGATCGTAAAGGCGAAG
TTTCTGACGGTCAGGAAGATTACATCCGTTGCGCGATCTACTACATCGAAAAAGGTA
ACGGTCGTGTTTACTCTAAATTCGACCCGAACTACGTTCGTTCTCTGAAACGTTTCT
CTGACAAAGGTATCATCCCGCCGCTGTCTGACGCGCAGGCTGAAGCTATCGAATTC
TTCGACCAGACCTGCTACAAAGAATCTATCGGTAACGTTCTGGAAGTTGGTGACGTT
CACTTCATGACCAACAACCACCTGTACCACTCCCGTCAGGCATACACTGATCACGAA
CCGCCGGCTCCGCGTCGTCACCTGCTGCGTCTGTGGGTTTCTACTCCGGAATCTG
AAGGTGGTTGGAAACTGCCGTACCACGATTCTGACTGGAAACGTCGTGGTGGTGTT
CAGGTTGATGACCGTCCGCACAAAGTTCTGCTGCACGCTGACTAA

**Protein Stock Concentration:** 1.26mM

**Storage/Assay Buffer:** 50mM TRIS, 50mM NaCl, 5% glycerol (w/w), pH 7.5

**DfmD Sequence**

ATGACTACCACCGCTGAAGCTTACCTGTCTATCGACTGGGGTTCCGGTGAAACCGG
TCGTTACCACTGGATCTGGCTGCGTGACTCTTGCCTGTGTGAAACCTGCCGTAACG
CTTTCGCTAAACAGAAATACTTCGATTCTGCTACCCTGCCGCTGGATATCCGTCCGC
GTTCTGTAACTCGTTCTGCTGAAAACGGTCTGGAAATTGTTTGGGAAGATGGCCAC
GAATCTCGTTATCCGGATTCTTGGCTGCGTGAACACTCTACCCCGGTTAAACCGTCC
CGCCCGGAACAGCGTTGGTCCCCGTGGTCTAGCGCTGAAGTGGTAGCTGATGGCA
CCTTCGCGCACGCTGATGTTATGGCGGATAACAAAGCTCTGGTTGGCGCTCTGGAA
CACCTGTTCCGTTATGGTCTGGTTGTTCTGCGTGGTACCGACGCTGAAGATGTTGAT
CCGGATGCTCTGTGCTCTCGTCTGGCGGGTTTCGTTGATCGTTCCTACTTCGGTGA
ATACTTCGATCTGGAAGTTAAACCGGACAACCGTACCGACTCTATCAGCTTCAGCAC
TCGCCAGCTGCCGCTGCACACTGACATCCCGTACTATTCTACCCCGCCGGATTACC
AGTTCCTGTTCGGTCTGGAAGTTAACGACGCTGCAACTGCTAGCCAGGGCGGTCGT
ACCCGTTTCGTTGACGGCGTGGCTGCGGCTCTGTCTCTGAAAGAACGTGACCCGG
AAGCGTTCGCGGTTCTGACCTCCACCGAAGTTATCTACCGTGCTGAATACGGTGAC
GCGGAAAAAATCTACCACCACCAGACCCCGGTTATCCACCTGAACAACGACGGTGA
AGTTGTTCGTCTGGTTAACAACCCGACCAAAATGTTCTTCGACAACGTTCCGTTCGA
TGAAGTGACCGGTGTTTACCGTGCGTACTCTGCGTTCAAAGCTCTGATGGACGAAG
AAGGTCGTGCTTATCACCACAGCTGGCGTCAGGGTGACATGATCATCTTCGATAACC
GTCGTATCTTCCACGGTCGTGAACAGTTCGATCAGACCGGTATGCGTCGTAAACTG
CGTGGTGGTTACTTCTCTGAAGTTGAACTGCGTGCGCGTTCTCGTTTCGCTGATGA
AA CCGTT

**Protein Stock Concentration:** 5.9mM (NMR Assay), 2.6mM (ESI-MS Assay)

**Storage/Assay Buffer:** 50mM HEPES, 50mM NaCl, 5% glycerol (w/w), pH 7.5